machines

MDPI

Review

A Cross-Scale Review of Thermodynamics-Dominated Cavitation and Failure Mechanisms in Liquid Hydrogen Pumps

Heng Xu [1,†], Xu Wang [2,†], Yi Fang [2], En-Ming Zhu [2], Ju Guo [2], Yi-Ming Dai [3], Ji-Chao Li [4] and Ji-Qiang Li [2,*]

[1] School of Engineering, Shandong Xiandai University, Jinan 250104, China
[2] School of Transportation, Ludong University, Yantai 264025, China
[3] Department of Electronic, Electrical and Systems Engineering, University of Birmingham, Birmingham B15 2TT, UK
[4] School of Mechanical Engineering, Jining University, Qufu 273155, China
* Correspondence: ljq7436@ldu.edu.cn
† These authors contributed equally to this work.

Abstract

The wide application of liquid hydrogen as a key energy carrier is severely limited by the reliability of high-pressure and low-temperature pumps. The traditional research on liquid hydrogen pumps relies on empirical analysis of isolated components, but fails to reveal the fundamental failure mechanism of these pumps. This review argues for a paradigm shift in the understanding and design of liquid hydrogen pumps. We systematically decomposed the failure of the liquid hydrogen pump into a thermodynamic-driven, cross-scale cascading process rather than the failure of isolated components. At the molecular level, the extreme thermal physical properties of liquid hydrogen (ultra-low latent heat and surface tension) can lead to widespread nucleation under slight thermal disturbances. At the mesoscopic scale, the initial perturbation is significantly amplified through the nonlinear dynamics of bubble clusters. This amplification is characterized by intense collapse and strong energy concentration due to the low density and low viscosity of liquid hydrogen. At the component level, this enhanced destructive energy will cause faults similar to phase transitions; namely, the liquid lubrication in the bearings will disappear, the seals will shift from viscous blockage to gas diffusion, and at the same time, the damage caused by low-temperature hydrogen cavitation and corrosion to the materials will also occur simultaneously. At the system level, the strong dynamic coupling among the subsystems has led to a nonlinear performance collapse. This cross-scale failure chain reveals the flaws in the classical cavitation theory, which is based on the assumptions of isothermal and inertia dominance. We have expounded the thermodynamic-dominated cavitation state in liquid hydrogen. This state is quantified by the Σ parameter and governs the multimodal behavior of low-temperature cavitation phenomena. To address this complexity, we have proposed a comprehensive framework that integrates multi-scale collaborative simulation and digital twin, combining molecular dynamics, CFD, system dynamics, and targeted experiments. This review proposes a candidate physical framework for addressing the reliability challenges of liquid hydrogen pumps. It also provides a clear roadmap for the next generation of inherently robust cryogenic fluid machinery, and offers a reference for the design of energy systems under other extreme conditions.

Keywords: liquid hydrogen pump; thermodynamic cavitation; cross-scale failure chain; multi-scale simulation; cryogenic fluid dynamics; hydrogen energy infrastructure

Check for updates

Academic Editor: Kim Tiow Ooi

Received: 9 April 2026
Revised: 18 May 2026
Accepted: 20 May 2026
Published: 28 May 2026

Copyright: © 2026 by the authors. Licensee MDPI, Basel, Switzerland. This article is an open access article distributed under the terms and conditions of the Creative Commons Attribution (CC BY) license.

1. Introduction

Liquid hydrogen possesses a high hydrogen density of 70.8 kg/m^3 and can be stored under near-atmospheric pressure (≈0.1 MPa), significantly enhancing the safety and economic feasibility of its storage and transportation [1–3]. Owing to its high volumetric energy density and low storage pressure, liquid hydrogen has emerged as a viable solution for large-scale, long-distance hydrogen transportation and is regarded as a critical medium in the future hydrogen supply chain [4]. In liquid hydrogen refueling stations and aerospace propulsion systems, high-pressure liquid hydrogen pumps serve as core power equipment, whose performance directly influences the efficiency and safety of the storage and transportation infrastructure. Under the extreme cryogenic condition of −253 °C (approximately 20 K), liquid hydrogen exhibits remarkable thermophysical properties, including an exceptionally low latent heat of vaporization, low viscosity [4,5], and low surface tension [6]. These extreme properties give rise to a series of cross-scale coupled challenges spanning from molecular-scale phase change to system-scale instability. These issues are interlinked and progressively amplified, thereby constituting a core bottleneck in the technological industrialization of liquid hydrogen pumps.

In recent years, review studies on liquid hydrogen pumps have demonstrated a clear evolutionary trajectory. Researchers have widely recognized that early reviews predominantly focused on isolated technical aspects, such as Qiu et al. [7] investigating unsteady heat transfer and fluid flow within the cylinders of reciprocating liquid hydrogen pumps and Lai et al. [8]. To address issues such as the insufficient hydraulic bearing capacity of high-speed liquid hydrogen centrifugal pumps and the instability of cavitation, both of which fall within the scope of local mechanism analysis. In contrast, recent studies have shifted toward system integration. Examples include Gao et al. [9], who systematically outlined the core technical challenges and co-optimization pathways for the domestic development of high-pressure liquid hydrogen pumps, and Wei et al. [10], who reviewed advances in high-pressure liquid hydrogen pumps from the perspective of multi-scale failure mechanisms and component coupling. This shift marks a transition from "component optimization" toward "system coupling." In addition, in terms of thermal management, the design and optimization of chemical heat pump systems such as alcohol–ketone–hydrogen systems also provide reference examples for efficient energy conversion and thermal enhancement [11,12], which offers cross-system references for the thermal management strategies of liquid hydrogen pumps in extremely low-temperature environments. In extreme application scenarios such as aerospace propulsion, the stable operation of the liquid hydrogen pump also needs to meet the thermal management requirements of the zero-evaporation storage system. Through the pump–heat pipe co-design, the loss of liquid hydrogen evaporation is suppressed [13]. This system-level integration approach further expands the research boundaries of the liquid hydrogen pump. However, the existing system-level reviews still focus on the comparison of macroscopic technical routes and the listing of performance parameters, and have not yet deeply dissected the cross-scale physical essence of fault transmission from material failure and component degradation to system instability [10,14]. This article was written precisely for this reason. It integrates the current research status and key technological breakthroughs in the high-pressure liquid hydrogen pump industry, and constructs a multi-scale theoretical framework.

Early reviews predominantly focused on limitations within isolated technical aspects such as cavitation simulation, material selection, or component design [7,8,15,16] (as summarized in Table 1). Against this backdrop, the research perspective has begun shifting toward system integration, thereby giving rise to review works undertaken from holistic, multi-dimensional viewpoints [9,10,17] (as shown in Table 2). Based on the comprehensive analysis of the existing results, this article holds that: The micro-level mechanism first

triggers the evolution at the meso-level; this evolution subsequently leads to the failure of key components; ultimately, the failure of these components causes the entire system to collapse. The understanding of how different levels couple and progressively trigger failure across scales is still insufficiently revealed. Second, there is an inadequate integration between the core technical challenges in the domestic development of high-pressure liquid hydrogen pumps—such as structural design, cryogenic insulation, and sealing control [9]—and corresponding engineering solutions. In particular, research on the co-optimization of liquid hydrogen pumps with associated components, such as superconducting motors [16] and pump–valve systems [18], is notably lacking. Finally, identifying practical and feasible pathways for breakthroughs that bridge theoretical advancements and engineering implementation requires further exploration considering recent industrial practices. This perspective distinguishes the present review from earlier reviews that focused primarily on isolated components or macroscopic technical summaries. Early studies [7,8] mainly focused on the optimization of isolated components and single-scale mechanical analysis based on classical cavitation theory. Recent system-level reviews [9,17] have systematically summarized the technical routes and performance parameters, but failed to deeply reveal the cross-scale physical essence of the failure propagation process. In contrast, this paper attempts to construct a quantifiable cross-scale failure chain, establish a thermodynamic-dominated cavitation model characterized by the Σ parameter, and propose corresponding multi-scale collaborative simulation methods. These efforts aim to make targeted adjustments in the analytical framework, research approach, and design thinking, rather than merely making local improvements. Examples include the flow characteristics of liquid hydrogen pumps under microgravity conditions [13], and the use of liquid nitrogen as an alternative medium for similar tests. Given the significant risks and high costs involved in conducting direct experiments with liquid hydrogen, this method is crucial for verifying the design of liquid hydrogen pump components [19,20].

Table 1. Technical Aspects Focused on in Early Review Studies of Liquid Hydrogen Pumps.

Author	Content of the Study
Qiu et al. [7]	The gas spring model was adopted to study the non-steady-state heat transfer and fluid flow in the cylinder of a reciprocating liquid hydrogen pump. The differences in heat transfer between liquid hydrogen and nitrogen during the compression process, the temperature distribution characteristics, and the influence of rotational speed on efficiency were analyzed. The effectiveness of the correlation formula in predicting the heat flux on the cylinder wall within a specific rotational speed range was verified.
Lai et al. [8]	The performance of hydrodynamic bearings for high-speed centrifugal pumps lubricated with liquid hydrogen was studied. An L-shaped coupling bearing structure was proposed. By optimizing and enhancing the load-carrying capacity of the journal bearing and thrust bearing, cavitation was effectively suppressed.
Li et al. [15]	Numerical simulation of the influence of suction temperature on the internal flow characteristics of hydrogen circulation pumps reveals the laws of pressure pulsation and leakage flow changes caused by temperature variations, and provides flow field distribution data within a specific temperature range.
Yim et al. [16]	Design a high-temperature superconducting axial flux motor suitable for high-pressure liquid hydrogen pumps. Through electromagnetic-mechanical coupling simulation, compare the mechanical stability of different coil types.

Table 2. System Integration Perspective in Recent Review Studies on Liquid Hydrogen Pumps.

Author	References (Year)	Research Emphasis
Gao et al. [9]	Natural Gas Industry, 2024, 44(8)	Systematically sort out the current research status of the high-pressure liquid hydrogen pump industry, focus on the core technical pain points, and propose engineering solutions and collaborative optimization ideas.
Wei et al. [10]	Fluid Machinery, 2022, 50(7)	Comprehensively review the research progress of high-pressure liquid hydrogen pumps, covering multi-scale failure mechanisms and key component adaptation technologies, and construct an overall cognitive framework of "component failure—system coupling".
Chen et al. [17]	Fluid Machinery, 2021, 49(9)	The research focuses on the reciprocating liquid hydrogen pump. It systematically summarizes the current research status of this pump in terms of structural design, thermal management, and sealing performance, and also looks forward to the directions of multi-physics field coupling optimization and engineering application.

To address the aforementioned challenges, this paper, building upon a systematic review of existing progress and incorporating the latest research findings from Gao et al. [9], Zhai et al. [14] and Chen et al. [17], aims to construct a more comprehensive and coherent cognitive framework and solution. It systematically constructed a complete causal chain of fault propagation, ranging from molecular-scale thermal disturbances to system-scale performance avalanches, thereby elucidating the dominant role played by thermodynamic effects in this process. Based on this foundation, the study proposes an integrated R&D methodology of "multi-scale collaborative simulation, experimental interactive validation, and digital twin-driven design," with the goal of overcoming the limitations inherent in traditional single-scale research. This study, by constructing a cross-scale understanding and solution framework for liquid hydrogen pumps, aims to provide a reference for the development of reliable and efficient liquid hydrogen pump technology. At the same time, it conducts a forward-looking analysis of the future trend of its application in engineering and its advancement towards intelligence.

2. Hydrogen Energy Industry Background and the Technological Positioning of Liquid Hydrogen Pumps

2.1. Global Energy Transition and the Strategic Value of Hydrogen Energy

The current world is confronted with two major severe challenges: one is the rapid depletion of traditional fossil energy reserves; the other is the continuous deterioration of the ecological environment. The instability of energy supply and the climate crisis caused by carbon emissions have become the core obstacles restricting sustainable development [21–27]. In this context, the "global energy transition" and the "carbon neutrality" goals have shifted from international initiatives to a collective action agenda, providing a clear framework and strong impetus for the development of clean energy [28,29]. For instance, as the world's largest energy consumer and carbon emitter, China has committed under the Paris Agreement to achieving carbon emissions peak by 2030 and increasing the proportion of non-fossil energy in primary energy consumption, demonstrating a firm alignment of its actions with national carbon neutrality goals [30].

Among the numerous clean energy options, hydrogen stands out for its unique advantages such as zero-carbon combustion, high energy density, and wide application scenarios [31]. It can be prepared through the electrolysis of water using renewable energy

(green hydrogen), produced by coupling carbon capture technology with fossil fuels (blue hydrogen), and can also be recovered and purified from industrial by-product hydrogen. Moreover, it can achieve multi-form conversion of electricity, heat, and gas. It is widely adaptable to the demands of multiple fields such as transportation, industry, and construction. In terms of the economic optimization of green hydrogen production, the scale-up and cost control of photovoltaic hydrogen production systems are among the key research directions. For instance, Okonkwo et al. [32] optimized the configuration of photovoltaic hydrogen production systems through HOMER software, analyzed the leveled hydrogen cost under different system architectures, and provided a technical and economic reference for the commercialization of green hydrogen production. Therefore, hydrogen energy is widely regarded as a strategic-level energy carrier for promoting energy transformation and achieving the vision of carbon neutrality [33,34].

Nevertheless, despite its significant strategic value, the global hydrogen energy industry remains at a nascent stage, facing substantial challenges spanning from production to application [35,36]. To achieve carbon neutrality goals, hydrogen energy has become a critical investment area in the global clean energy transition, with 65 countries having formulated national hydrogen strategies as of 2025. However, assessments by the International Energy Agency (IEA) indicate that the decarbonization efforts within the current hydrogen industry are significantly lagging. The majority of hydrogen production still relies on fossil fuels, with low-carbon hydrogen (encompassing both green and blue hydrogen) accounting for less than 1% of the total global hydrogen output [33]. This highlights the formidable challenges and urgency of transforming the energy structure. Concurrently, the nearly 2000 existing and planned low-carbon hydrogen projects globally, if fully implemented, could cumulatively make a substantial contribution to achieving deep decarbonization targets [37].

In its 2025 Global Hydrogen Review, the IEA systematically diagnosed the core bottlenecks hindering the scale-up of the current hydrogen industry. The report identifies insufficient cost competitiveness, ambiguous end use demand signals, underdeveloped regulatory frameworks, and lagging infrastructure as collective barriers impeding the transition of low carbon hydrogen from demonstration projects to commercial deployment. To address these structural obstacles, the report reveals a clear global policy consensus and actionable pathway: governments worldwide are strategically combining demand side incentives (such as sectoral quotas and mandatory targets), supply side support (including tax credits and direct subsidies), and infrastructure investment to systematically reduce investment risks, create initial markets, and steer capital flows. IEA's analytical framework provides an authoritative benchmark and theoretical foundation for this study to understand the evolving logic of global hydrogen policy instruments, assess their effectiveness, and distinguish the similarities and differences among regional models [33]. Figure 1 summarizes five key indicators from the IEA's 2025 assessment, including project realization risks, production costs, demand by sector, and electrolyser capacity trends. The industrialization of hydrogen is intrinsically linked to building a future clean, secure, and efficient energy system and achieving deep decarbonization goals. Within this process, overcoming key technical bottlenecks such as hydrogen storage and transportation carries strategic urgency. Among them, the liquid hydrogen pump, as the core equipment for efficient storage, transportation and distribution, significantly influences the feasibility of hydrogen energy in high-end applications. For instance, in heavy duty fuel cell vehicle refueling, liquid hydrogen pumps enable rapid filling at flow rates up to 285 kg/h and pressures of 45 MPa, supporting continuous refueling processes compliant with the SAE J2601 2 standard [38], thereby providing a reliable technical foundation for commercial operation. In aerospace propulsion systems, liquid hydrogen pumps serve as

critical components for cryogenic propellant delivery, where their cavitation characteristics and thermodynamic effects significantly influence engine performance and reliability. Therefore, in depth research and optimization of pump valve dynamic behavior, durability, and cryogenic cavitation flow in liquid hydrogen pumps are not only key to advancing hydrogen storage and transportation technology but also essential for enabling the large scale application of hydrogen in sectors such as transportation and aerospace [18,38–40].

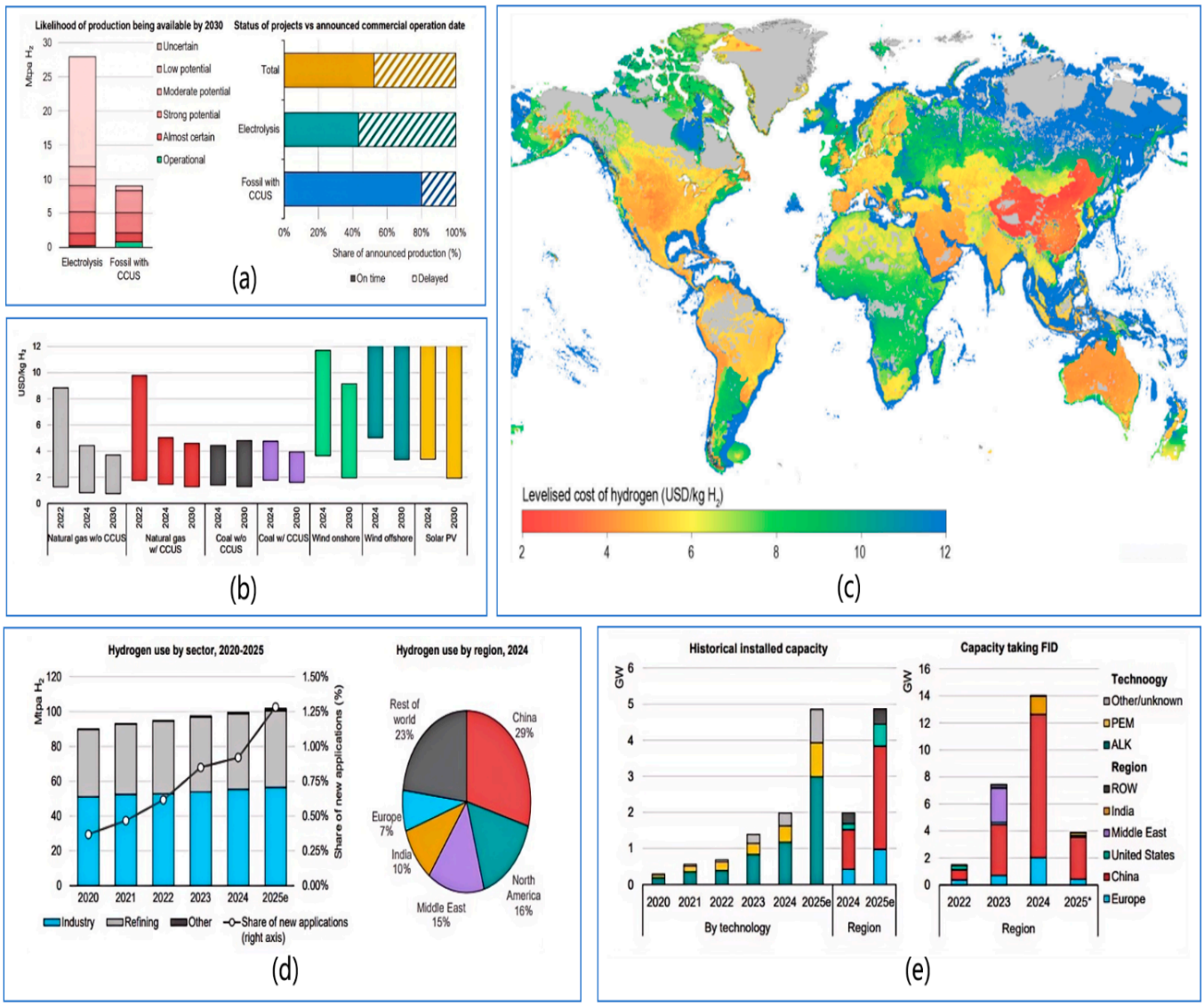


Figure 1. Overview of key indicators for the global hydrogen industry [33]: (**a**) Status and risk of low-emission hydrogen projects based on technology in 2030, (**b**) Status and risk of low-emission hydrogen projects based on regions in 2030, (**c**) Cost of electrolysis-based hydrogen production: Hybrid photovoltaic + onshore wind energy and offshore wind energy (STEPS, 2030), (**d**) Hydrogen demand in various industries and regions from 2020 to 2025, (**e**) Installed capacity of electrolyzers by technology and region (2020 to 2025) and feasibility study capacity (2022 to 2025).

2.2. Current Status of Hydrogen Energy Industry Development and the Pivotal Role of Liquid Hydrogen Storage and Transportation

Against the backdrop of the in-depth advancement of the global carbon neutrality strategy, hydrogen energy, as a key component of the clean energy system, is accelerating its transformation from policy guidance to market-driven, becoming the core track of global energy structure adjustment. Between 2021 and 2024, the global investment scale in the

hydrogen energy sector increased nearly eightfold, and the planned installed capacity of electrolyzers expanded ninefold. The industry's heat and resource agglomeration effect continued to stand out [26]. According to the data from "Global Hydrogen Review 2024", this growth trend is highly consistent with the global investment trend in low-emission energy, reflecting that the core position of hydrogen energy in the energy transition has reached a consensus [26]. From the perspective of the trend of technical route layout, global low-emission hydrogen production projects have formed two parallel models: one is hydrogen production using renewable energy; the other is hydrogen production using fossil fuels combined with carbon capture and storage technology. The former relies on the grid connection of large-scale clean energy (such as wind energy and solar energy), while accelerating the reduction in electrolysis technology costs and the improvement of industrial supporting facilities. The latter expands its coverage by leveraging the mature path of clean transformation of traditional energy and the advantages of reusing existing infrastructure. The two types of technologies complement each other in terms of resource matching, cost structure, and scene application, jointly promoting the continuous optimization of the hydrogen energy supply structure towards low-carbonization and diversification [41]. Particularly crucial is that the completion rate of the final investment decision (FID) for low-emission hydrogen projects has significantly improved. In 2023, the global capacity of low-emission hydrogen FID doubled to 3.4 million tons per year compared to the previous year, with electrolytic hydrogen production contributing 1.9 million tons per year and CCUS hydrogen production contributing 1.5 million tons per year. This marks that the industrialization of hydrogen energy has moved from the planning stage to a substantive implementation process [26].

In the hydrogen energy industry chain, the storage and transportation link, as a key hub connecting upstream production and downstream application, its technological maturity and cost control level directly determine the boundary of large-scale promotion of the hydrogen energy economy [1,42]. Liquid hydrogen, with its advantages of high energy density and low storage pressure, has become the optimal technical solution for large-scale and long-distance hydrogen storage and transportation, significantly reducing the unit hydrogen transportation cost and system space occupation. This conclusion has been verified by several industry studies. For example, the simulation analysis in "Collaborative optimization of hydrogen energy systems" shows that the unit energy consumption of liquid hydrogen storage and transportation is reduced by more than 30% compared with that of pressurized hydrogen [42]. However, the cryogenic nature of liquid hydrogen brings multiple extreme physical property challenges. Its extremely low latent heat of vaporization, low viscosity and low surface tension have caused multi-scale technical problems in the design and operation of key equipment in liquid hydrogen systems. Among them, the performance optimization of high-pressure liquid hydrogen pumps has become the core bottleneck restricting system efficiency [10,39].

During the storage and transportation of liquid hydrogen, "evaporation loss" is prone to occur due to factors such as external heat infiltration and heat release from the conversion of normal and secondary hydrogen, which poses strict requirements for the insulation design of storage tanks and the thermal management of the system [43,44]. A.M. Al-Orabi et al. found in the study of the Green hydrogen project in Egypt that the evaporation loss caused by heat infiltration could account for 5–8% of the total liquid hydrogen reserves, directly pushing up the storage and transportation costs [43]. To suppress the evaporation of liquid hydrogen, the zero evaporation (ZBO) storage system works in coordination with the liquid hydrogen pump through heat pipes to actively remove the heat inside the tank. Studies have shown that the nozzle flow rate of the pump has a crucial impact on the uniformity of the internal temperature of the storage

tank. Increasing the flow rate can significantly enhance the fluid circulation and reduce the maximum temperature, thereby providing important basis for system optimization [13]. As the core pressurizing equipment in liquid hydrogen refueling stations, high-pressure liquid hydrogen pumps need to operate stably under extremely low-temperature conditions of approximately 20 K (−253 °C) and achieve pressurization of liquid hydrogen from about 0.2 MPa to over 70 MPa. This type of pump generally adopts a reciprocating structure. Its technical challenges mainly focus on cooling, sealing and cavitation control: the viscosity of liquid hydrogen is extremely low, and the material has a large shrinkage difference at low temperatures, which is prone to seal failure and leakage. Meanwhile, cavitation is prone to occur during the inhalation process, which seriously affects safety and lifespan. To this end, technically, the main approaches are to enhance insulation by adding vacuum jackets, achieve pre-compression and degassing through multi-chamber design, and optimize self-lubricating sealing materials and structures. At present, commercial products (such as Linde, ACD, Cryostar) can achieve an output pressure of 87.5 MPa and a flow rate of approximately 1.55 kg/min, significantly outperforming hydrogen compressors in terms of energy consumption. However, their high cost and structural complexity remain constraints for large-scale application [10]. Liquid hydrogen technology still faces bottlenecks such as high liquefaction energy consumption, difficulty in controlling long-term storage losses, and lagging research and development of low-temperature adapted materials. These factors jointly restrict its large-scale commercial application process [9].

As of June 2023, a total of 1089 hydrogen refueling stations have been built worldwide. Among them, China has 351 stations, but they still mainly rely on gas hydrogen storage and transportation. The proportion of liquid hydrogen storage and transportation type refueling stations in foreign countries has reached nearly one-third [9,45]; this gap is attributed to multiple factors such as reliance on imported core technology equipment, low patent proportion, incomplete standard system, and higher production costs. The levelized cost of hydrogen from renewable energy in China is expected to drop to between $2.5 and $3.0 per kilogram by 2040. This is driven by the decline in the cost of renewable electricity and the reduction in the cost of electrolyzers. Regions with abundant solar resources, such as the northwest of China, will have the lowest production costs [46]. Apart from these macroscopic differences, during the vehicle refueling process, the liquid hydrogen pump also encounters some specific engineering challenges.

To address the specific engineering challenges faced by the hydrogen liquid pump during vehicle refueling, the industry has proposed and verified innovative solutions. For instance, a study [38] successfully met the requirements of the J2601-2 standard by adopting an integrated design that combines an immersed hydrogen liquid pump, a hydraulic drive unit, and a direct refueling loop. The pre-cooling function of this scheme is achieved through a PID control shunt circuit, which can precisely control the hydrogen injection temperature to −40 °C. No separate refrigeration device is required. It significantly enhances the stability and reliability of the system under continuous and rapid filling conditions. This provides a beneficial technical solution for addressing related engineering issues. Figure 2 is adapted from Ref. [34], which analyses global hydrogen innovation trends based on patent data. As shown in Figure 2a,b, between 2011 and 2020, Europe and Japan led international patenting in hydrogen technologies, with strong revealed technology advantages across most value chain segments. Figure 2c maps the geographic distribution of hydrogen innovation clusters, highlighting major hubs in Europe (e.g., Paris, Munich) and Asia (e.g., Tokyo, Seoul) [34].

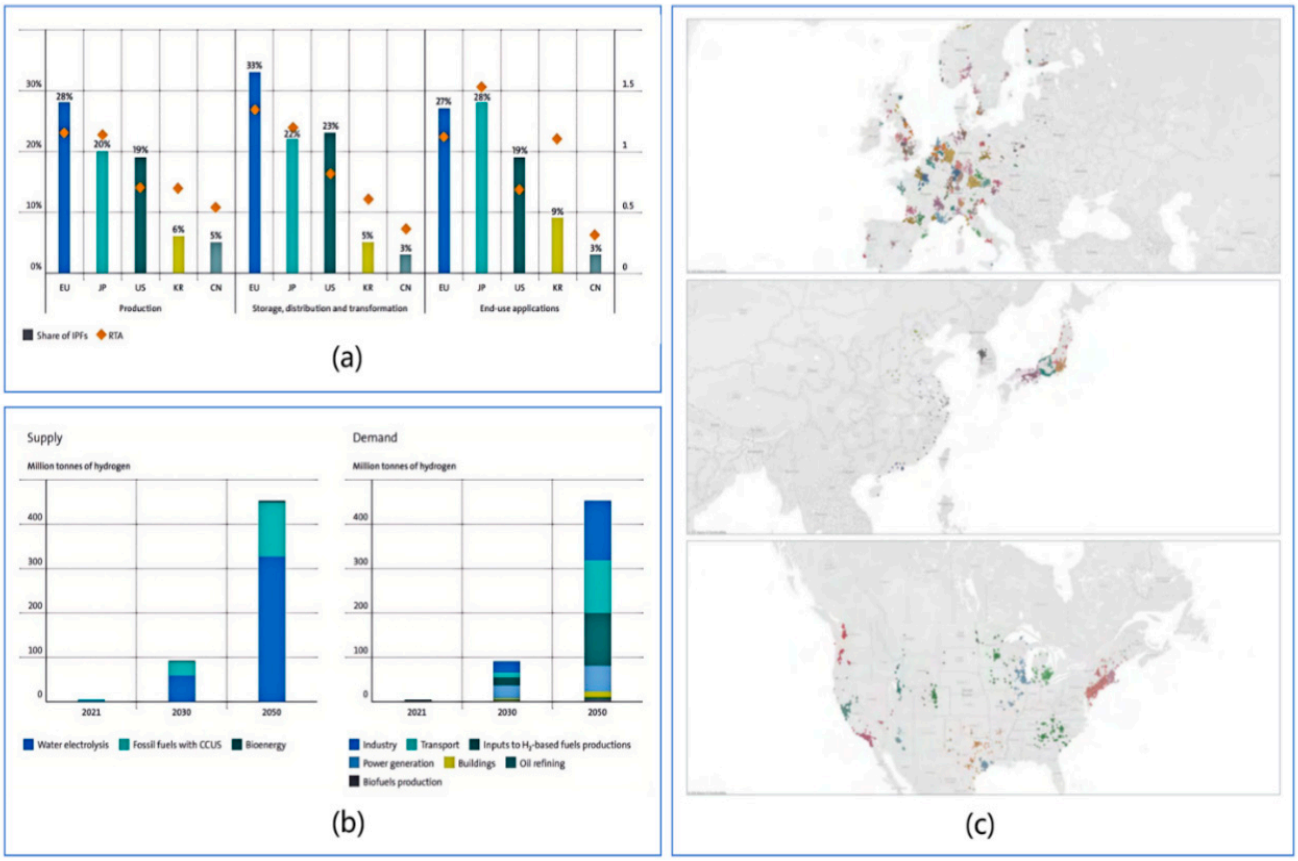


Figure 2. Evolution of Sectoral Shares and Supply–Demand Structure in the Global Hydrogen Energy Supply Chain [34]. (**a**) Share of international patenting and revealed technology advantage by main world regions and value chain segments. (**b**) Share of international patenting and revealed technology advantage by main world regions and value chain segments. (**c**) Global distribution of hydrogen innovation clusters (IPFs, 2011–2020).

2.3. Core Characteristics of Multi-Scale Technical Challenges in Liquid Hydrogen Pumps

As the core power unit of the liquid hydrogen energy system, the working medium inside the liquid hydrogen pump is liquid hydrogen. It possesses extremely extreme thermal physical properties, including an extremely low boiling point, a high latent heat of vaporization, and a significant orthogonal–parallel hydrogen conversion heat release. These characteristics not only influence the cryogenic fluid dynamic behavior of the pump but also pose severe challenges to its thermal management, structural materials, and system efficiency [1,47]. The extreme properties of liquid hydrogen (such as its very low boiling point and ortho–para conversion heat release) can trigger cavitation and intense phase change at microscopic flow scales, subsequently inducing mesoscale flow instabilities and strong pressure pulsations. During the storage and transportation of liquid hydrogen, thermal stratification leads to a significant "self-pressurization" effect. If not controlled via venting or active cooling, the system pressure will rise sharply. This not only increases the safety risk for storage tanks but also causes pressure fluctuations and an unstable gas–liquid interface that severely disrupts the stable operation of downstream pumps [36]. The physical properties of liquid hydrogen, such as its very low density and viscosity, make it more prone to flow instabilities like cavitation and two-phase flow during transport. This unstable flow state, combined with hydrogen's inherent tendency to cause hydrogen embrittlement in metals, poses even more severe challenges to the long-term performance of critical components such as bearing lubrication reliability and dynamic seal integrity within pump and valve systems [47]. Therefore, the design and operation of liquid hydrogen

pumps must comprehensively consider these multi-scale, multi-physics coupling effects to enhance system reliability and control precision.

The thermal management challenges faced by liquid hydrogen pumps and the heat generation mechanisms of their bearings exhibit non-negligible coupling effects in driving the aforementioned multi-scale issues. Research in this field primarily focuses on core areas such as bearing frictional heat generation mechanisms, heat conduction pathways under extreme operating conditions, the influence of thermal disturbances on fluid properties, and the coupled effects of cavitation and heat transfer [7,48,49]. Traditional research methods have accumulated considerable knowledge in coupling analysis, lubrication failure characterization, and simulation, but these findings are largely based on conventional operating conditions and working media. Under the extreme conditions such as extremely low temperatures and high-speed rotation faced by the liquid hydrogen pump, it is difficult for the system to conduct detailed thermal management and effectively suppress heat generation. Therefore, systematic research on multi-scale thermal management and heat suppression is still insufficient. In particular, the chained multi-physics coupling mechanism involving "bearing frictional heat, environmental heat leakage, liquid hydrogen phase change, and cavitation induction" still lacks comprehensive investigation, and no universal thermal management design guidelines applicable to liquid hydrogen pumps have yet been established [7]. In microgravity environments, the weakening of buoyancy effects exacerbates thermal stratification within liquid hydrogen storage tanks. Three-dimensional numerical simulations indicate that optimizing the arrangement of pump-nozzle units and adjusting nozzle flow velocity can effectively guide the cooling flow field, improve temperature uniformity, and thereby enhance the performance of Zero Boil-Off storage systems. This active thermal management strategy under special environmental conditions further expands the research dimension of thermal control for liquid hydrogen storage systems in microgravity scenarios such as aerospace applications [13].

3. Cross-Scale Challenges and Causality Chain of Liquid Hydrogen Pumps

As pointed out in Chapter 2, the extreme physical properties of liquid hydrogen not only constitute the physical background for component failure but also are the deep-seated root cause that triggers the system-level performance avalanche. On this basis, this chapter will further reveal how this process is scaled up step by step along the scale chain of "molecule → mesoscopic → component → system", and clarify the core role of thermodynamic effects in it. As indicated in the preceding discussion, the extreme thermophysical properties of liquid hydrogen are not merely the background for component failures but the root cause triggering systemic collapse. The failure of a liquid hydrogen pump is, in essence, a "domino effect" chain reaction that originates from molecular-scale thermal perturbations and culminates in a system-wide performance avalanche. This section aims to reveal and establish a causal chain of cross-scale fault propagation and energy amplification: molecular thermal sensitivity → microscopic cavitation → mesoscopic flow instability → component mechanical failure → system performance collapse. At the same time, it clarifies the dominant role of thermodynamic effects in this chain. This causality chain not only possesses a clear direction of dynamic propagation but also achieves nonlinear energy amplification at the mesoscale and component scale, ultimately leading to an avalanche-like degradation of system performance.

3.1. Molecular/Microscopic Scale (Property Origins): Extreme Thermophysical Properties and Thermal Disturbance Sensitivity of Liquid Hydrogen

Based on the homogeneous nucleation theory articulated by Brennan [50], the nucleation rate is highly sensitive to surface tension and latent heat of vaporization. Liquid hydrogen exhibits extreme values in both of these properties: its exceptionally low latent heat of vaporization and surface tension [6,51,52] result in an extremely low nucleation energy barrier. Theoretical analysis indicates that, under such physical properties, the energy density provided by inevitable microscale thermal disturbances within the system—such as bearing frictional heat or ambient heat leakage—readily exceeds this nucleation barrier. Consequently, homogeneous nucleation cavitation becomes a typical and easily triggered phase change mode in liquid hydrogen systems [50]. The study by Qiu et al. [7] on heat transfer processes of liquid hydrogen in enclosed cylinders further reveals the complexity and importance of such thermodynamic processes within liquid hydrogen pumps. Thus, liquid hydrogen systems are extremely sensitive to minor thermal flow perturbations, suggesting that homogeneous nucleation may play a much more significant role in liquid hydrogen than previously assumed. Molecular scale phase change acts as the "trigger" for all subsequent issues.

Liquid hydrogen exhibits an extremely low boiling point under standard atmospheric pressure. According to authoritative thermophysical data from NIST, its corresponding volumetric latent heat of vaporization at this temperature is also remarkably low. Compared to the volumetric latent heat of vaporization of water under ambient pressure, there exists a substantial difference in orders of magnitude between the two, with the former being only about one tenth to one twentieth of the latter [6,51]. This extreme disparity highlights the essential characteristic that liquid hydrogen requires very low energy density for vaporization. From a microscopic perspective, the onset of phase change can be understood as a nucleation process triggered by random thermal fluctuations, where a sufficient energy fluctuation enables a collective of molecules to overcome intermolecular forces and form a critical nucleus [53].

According to cavitation theory, the inception of cavitation begins with the formation and growth of vapor nuclei within the liquid [50]. Surface tension plays a decisive role in this process, constituting an energy barrier; a vapor nucleus can only stabilize and develop into a visible cavitation bubble when the local pressure drops sufficiently to overcome this barrier [54]. The extremely low surface tension of liquid hydrogen implies that the energy cost required to form a gas–liquid interface is minimal. This directly results in a highly unstable liquid phase, where even diminutive energy fluctuations are adequate to trigger the formation and growth of cavitation nuclei [50,53].

The unique extreme thermophysical properties of liquid hydrogen constitute the fundamental physical cause for its exceptionally sensitive and intense cavitation behavior. On the one hand, its extremely low volumetric latent heat of vaporization implies an extremely low "energy density" required for phase change. On the other hand, its exceptionally low surface tension significantly reduces the energy barrier for forming a gas–liquid interface [6,51]. Under the coupled effect of these two properties, the energy supplied by small, inevitable thermal-flow disturbances within the system (such as bearing frictional heat or environmental heat leakage) is sufficient to overcome the very-low phase-change energy barrier and trigger large-scale homogeneous nucleation cavitation [9]. This extremely low thermodynamic threshold represents the core physical mechanism underlying the high sensitivity to disturbances and the rapid development of cavitation in liquid hydrogen systems.

On the other hand, multiple micro disturbance sources inevitably exist within the system, which are of critical importance for liquid hydrogen due to its extreme thermal

sensitivity. First, bearing friction heat is an inherent thermal source in rotating machinery, and the generated heat is conducted into the working fluid through the shaft and housing [48,55]. Second, environmental heat leakage constitutes a fundamental challenge in cryogenic systems; despite insulation measures, heat ingress driven by the substantial temperature difference cannot be entirely eliminated [56–58]. This study contends that these two persistent, albeit small, heat fluxes collectively serve as a potential effective energy source for triggering cavitation in liquid hydrogen.

It is noteworthy that in a system with an extremely low thermodynamic threshold, even the minute energy deposited by high-energy particles such as cosmic rays in the medium may become a non-negligible disturbance source. Existing research has demonstrated that such energy deposition is sufficient to trigger nucleation events in cryogenic fluids like superfluid helium [59,60]. Given that liquid hydrogen similarly possesses an extremely low volumetric latent heat of vaporization, such effects could significantly influence the sensitivity of cavitation inception in liquid hydrogen.

The fundamental distinction between conventional fluids and liquid hydrogen lies in the magnitude of their thermodynamic stability thresholds—specifically, the energy barrier that resists minor thermal disturbances and prevents phase change differs by orders of magnitude. Conventional fluids such as water typically exhibit relatively high specific heat capacity and thermal diffusivity. A higher specific heat capacity implies a smaller temperature rise for the same amount of absorbed heat [61], while higher thermal diffusivity enables rapid dispersion of localized heat across the entire flow field, thereby effectively dampening the formation of local hot spots [62]. The combined action of these two properties makes it difficult for conventional fluids to reach the stringent localized thermodynamic conditions required for homogeneous nucleation.

However, the unique thermophysical properties of liquid hydrogen lead to a fundamentally different response to thermal disturbances compared to conventional fluids. Due to its extremely low volumetric latent heat of vaporization and surface tension, its phase-change energy barrier is reduced to an exceptionally low level [51,53]. Under such conditions, minor thermal pulses, such as those from bearing friction or environmental heat leakage, are no longer negligible noise [7]. According to homogeneous nucleation theory, the energy supplied by these disturbances is already sufficient to instantaneously generate a multitude of vapor nuclei within the bulk liquid hydrogen [50]. Similarly, in the field of high-energy physics, the minimal energy deposited by particles such as cosmic rays in cryogenic fluids like superfluid helium has been confirmed as an effective mechanism for triggering nucleate boiling [59]. This analogy strongly suggests that in liquid hydrogen, the pervasive, microthermal disturbance-triggered homogeneous nucleation cavitation constitutes the core mechanism underlying the high sensitivity and severity of its cavitation issues.

This indicates a fundamental shift in the cavitation inception mechanism in liquid hydrogen. Cavitation no longer relies on preexisting heterogeneous nucleation sites common in conventional fluids, such as solid surface defects or suspended particles, but originates from spontaneous and intense homogeneous nucleation processes within the bulk liquid itself. In conclusion, under the actual operating conditions of the liquid hydrogen turbine pump (such as high rotational speed accompanied by heat generated by bearing friction and heat leakage from the environment), uniform onset cavitation is not an accidental event but rather an expected and recurring phenomenon.

Cavitation exhibits strong non-isothermal characteristics in liquid hydrogen. According to the classical cavitation theory [50], the growth of cavitation bubbles cools the interfacial liquid by absorbing the latent heat of vaporization, while the latent heat of condensation released when they collapse heats the liquid. This intense latent heat exchange

constitutes a thermodynamic inhibition effect, which significantly alters and inhibits the dynamic behavior of cavitation bubbles. According to Hord's classic experimental research, the intense latent heat exchange during the cavitation process of liquid hydrogen leads to a significant local temperature drop at the cavitation bubble interface, thereby triggering a strong thermodynamic inhibitory effect. This cavitation kinetics dominated by thermodynamic scale effects is fundamentally different from the cavitation of normal-temperature media (such as water) dominated by inertial forces [63]. The simulation through the dual-distribution function multiphase lattice Boltzmann method (DDF-MLBM) revealed that the peak core temperature and pressure during the collapse of liquid hydrogen bubbles were significantly higher than those of liquid nitrogen, and the collapse time was shorter, further confirming the significance of the non-isothermal effect [64].

Consequently, the intense thermodynamic effects (i.e., non-isothermal cavitation) observed in liquid hydrogen cavitation stem fundamentally from its extreme molecular-scale thermophysical properties: the combined action of extremely low latent heat of vaporization and surface tension renders liquid hydrogen highly sensitive to microthermal disturbances, facilitating phase change initiation. It is precisely this intrinsic microscopic property that fundamentally dictates the distinctive macroscopic cavitation bubble dynamics observed in its flow behavior.

This extreme sensitivity can be rigorously quantified using classical nucleation theory. The steady-state homogeneous nucleation rate, J is given by:

$$J = J_0 exp\left(-\frac{\Delta G_{crit}}{k_B T}\right) \tag{1}$$

where J_0 is a kinetic prefactor, k_B the Boltzmann constant, and T the absolute temperature. The critical energy barrier for nucleation, ΔG_{crit}, is expressed as:

$$\Delta G_{crit} = \frac{16\pi\sigma^3}{3(\Delta P)^2}, \Delta P = \frac{\rho_v L_v \Delta T}{T} \tag{2}$$

For a fixed T and ΔT, $\Delta G_{crit} \propto \sigma^3/(\rho_v L_v)^2$. According to NIST data [6], liquid hydrogen at 20 K exhibits $\sigma \approx 2.3 \times 10^{-4}$ N/m and $\rho_v L_v \approx 1.4 \times 10^6$ J/m^3, both approximately two orders of magnitude lower than those of water. Substituting these values yields an exponentially reduced ΔG_{crit}, resulting in a dramatically increased J. This mathematical result confirms that even minor thermal disturbances, such as the heat generated by bearing friction or environmental heat leakage, are sufficient to trigger widespread and uniform nucleation phenomena in liquid hydrogen. According to classical nucleation theory, the critical energy barrier for uniform nucleation in liquid hydrogen is estimated to be many orders of magnitude lower than that in water, which means it is extremely sensitive to thermal disturbances.

3.2. Mesoscale (Energy Amplification): Nonlinear Evolution of Cavitation Bubble Clusters and Flow Instability

According to cavitation and multiphase flow theory, while cavitation originates from microscopic vapor nuclei, its energy amplification and systemic impact primarily occur at the mesoscale [50]. At this scale, bubble clusters undergo nonlinear evolution and coalescence, transforming molecular-scale phase-change events into observable macroscopic effects [50,63]. Energy amplification refers to the physical process that occurs within the mesoscopic scale of the liquid hydrogen pump. During this process, the initial perturbation energy generated by the phase transition at the molecular scale is significantly enhanced in the local energy density through the nonlinear evolution of bubble clusters and the coordinated collapse of bubble groups. This is the distinctive mesoscopic feature that

distinguishes liquid hydrogen cryogenic cavitation from that of normal temperature fluids. Based on the measured data published by Ezzatneshan et al. in 2024 [64], under the same boundary conditions ($\lambda = 1.5$, $\theta = 30^\circ$), the peak core pressure of liquid hydrogen cavitation collapse is 1.93 times that of liquid nitrogen, the peak core temperature is 1.75 times that of liquid nitrogen, and the collapse time step of liquid hydrogen (approximately 600) is much shorter than that of liquid nitrogen (approximately 850). These three parameters constitute the verifiable criterion of "significant energy amplification effect". Compared to conventional media like water, cavitation in liquid hydrogen exhibits significantly intensified unsteady characteristics [64]. The physical basis for this assertion stems firstly from the extremely low density and dynamic viscosity of liquid hydrogen, both of which are substantially lower than those of water. This theoretically leads to a higher dynamic response frequency of bubbles and reduced flow damping, inevitably giving rise to more violent cavitation dynamics.

Figure 3 clearly demonstrates the significant differences in bubble collapse dynamics between liquid hydrogen (LH_2) and liquid nitrogen (LN_2) through numerical simulation results. Under identical boundary conditions (e.g., distance ratio $\lambda = 1.5$, contact angle $\theta = 30^\circ$), the LH_2 bubble exhibits considerably more violent collapse characteristics than the LN_2 bubble. Specifically, the collapse time for LH_2 ($t = 600$) is notably shorter than that for LN_2 ($t = 850$), indicating a faster and more concentrated energy release process. At the moment of collapse, the maximum induced jet velocity for LH_2 substantially exceeds that for LN_2, confirming the formation of a more energetic and erosive micro-jet in liquid hydrogen, which poses a more severe threat to adjacent surfaces. More importantly, the comparison of thermodynamic parameters recorded during the collapse process is particularly striking. The core region of the LH_2 bubble reaches higher maximum temperature and maximum pressure values, approximately 1.75 and 1.93 times those of the LN_2 case, respectively. This phenomenon directly substantiates the existence of more pronounced "local hot spots" and stronger pressure pulses in liquid hydrogen cavitation.

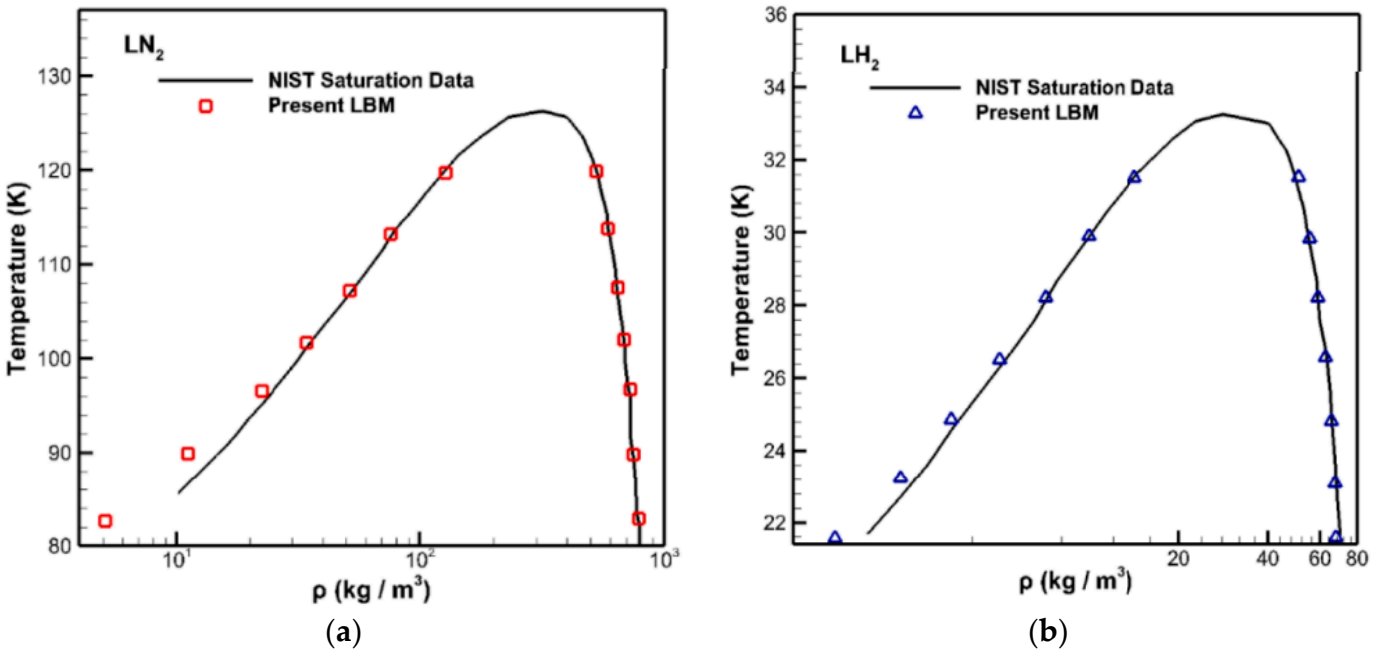


Figure 3. Consistency of the current numerical results was validated against the analytic Maxwell construction: (**a**) liquid nitrogen, (**b**) liquid hydrogen [64].

The underlying reason for these phenomena lies in the unique thermophysical properties of liquid hydrogen, such as its extremely low density, viscosity, and specific heat

capacity, which render it more sensitive to thermodynamic effects during the phase change process. During bubble collapse, the intense compression causes a sharp rise in gas temperature, while the lower thermal inertia of liquid hydrogen makes the energy less readily dissipated, thereby resulting in higher localized temperature and pressure peaks and more violent overall cavitation dynamics.

Furthermore, given the highly flammable and explosive nature of liquid hydrogen itself, along with its extremely low boiling point, experimental research on its cavitation flow faces significant challenges in terms of safety and cost [10]. Therefore, most current studies use liquid nitrogen, a medium that is safer and has similar thermal physical properties (such as low density and low viscosity) to liquid hydrogen, to investigate the general flow behavior of low-temperature cavitation [65–67]. Existing liquid nitrogen cavitation experiments have clearly demonstrated that its cavitation structures appear more fragmented compared to those in ambient temperature media such as water, and the intensity of flow field pressure pulsations is significantly enhanced [65]. These related studies collectively point to a definitive conclusion: cavitation in liquid hydrogen exhibits far more pronounced unsteady characteristics than in conventional media [10,64].

Experimental and numerical studies utilizing liquid nitrogen as a substitute medium have yielded a key consensus: cryogenic cavitation structures exhibit a markedly "mushy," fragmented morphology, and their dynamic behavior demonstrates a high sensitivity to thermodynamic effects, displaying far stronger unsteadiness than that observed in ambient-temperature media [65,67]. These phenomena are fundamentally attributed to the strong temperature dependence of key properties such as saturated vapor pressure and density (specific volume).

Building upon this consensus, this study further elucidates that the extreme unsteady characteristics exhibited by liquid hydrogen cavitation are fundamentally rooted in its uniquely ultra-low density and ultra-low viscosity [6,51]. These two core thermophysical parameters dominate the cavitation dynamics through two key pathways: low density notably increases the dynamic response frequency of bubbles, while low viscosity substantially weakens the damping effect of the flow field [64]. The phase change energy released during bubble inception and collapse at the microscopic scale is effectively concentrated, transmitted, and amplified through the collective nonlinear dynamics of bubble clusters at the mesoscopic scale [50]. It is precisely this mesoscale energy amplification process that ultimately manifests as flow instability, intense pressure pulsations, and high-frequency noise at the macroscopic scale in systems such as pumps.

Figure 4 presents the physical image of the cross-scale evolution in the cavitation phenomenon. This paper comprehensively analyzes the numerical simulation results focusing on different aspects. Studies have shown that macroscopic attached cavities break and fall off under the influence of reentry jets and other factors, forming mesoscopic-scale cloud-like cavitation clusters, which eventually break into discrete microscopic bubble groups during transportation. This evolution chain of "macroscopic cavities $\rightarrow$ mesoscopic cloud clusters $\rightarrow$ microscopic bubble clusters" (as shown in Figure 5) visually reveals the dynamic evolution process of cavitation structures across multiple spatial scales. Through multi-scale simulation, it was found that the bubble size distribution (BSD) within cloud-like cavitation exhibits a double-power law characteristic: the small bubble spectrum follows the $-\frac{4}{3}$ power law, and the large bubble spectrum follows the $-\frac{10}{3}$ power law. Moreover, this rule is not affected by the number of cavitation phenomena. This quantitative feature provides a key basis for the modeling of mesoscopic-scale cavitation evolution.

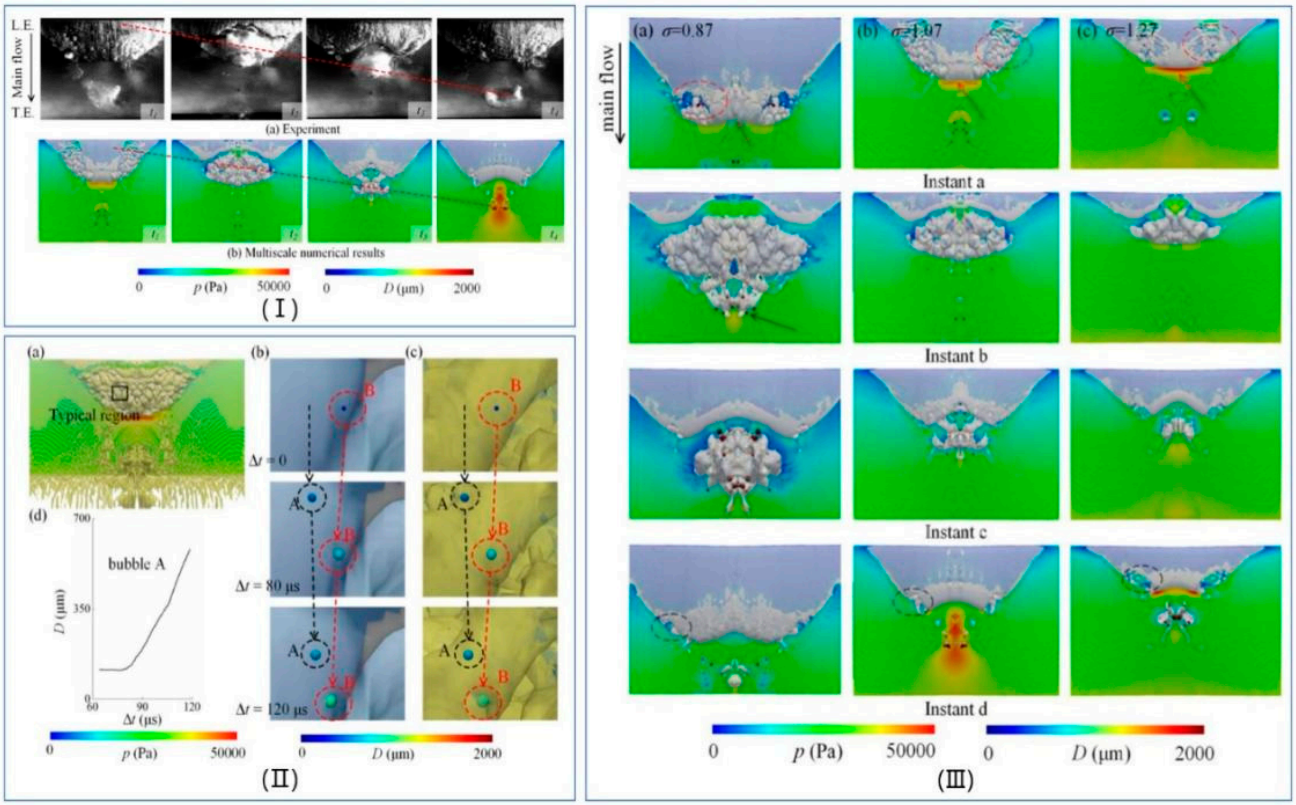


Figure 4. Schematic diagram of the cross-scale evolution of liquid hydrogen cavitation structure: "macroscopic cavity—mesoscopic cloud clusters—microscopic bubble clusters" [68].

The energy amplification effect of liquid hydrogen cavitation has been confirmed by numerical simulation: Ezzatneshan et al. [64] simulated the collapse of liquid hydrogen bubbles using the lattice Boltzmann method and found that under the same boundary conditions, the collapse time of liquid hydrogen bubbles was shorter than that of liquid nitrogen, and the jet velocity, core temperature and pressure were 1.55 times, 1.75 times and 1.93 times that of liquid nitrogen, respectively (T_0 = 20 K, P_0 = 0.1 MPa). Lai et al. [8] conducted a detailed numerical simulation of the multi-physical field coupling of heat, flow and cavitation, combined with the design of the coupling structure and the optimization of system parameters. From both the principle and application perspectives, they verified that in high-speed liquid hydrogen-lubricated bearings, by carefully designing the mesoscopic-scale flow channel structure and phase change conditions, the hydrodynamic pressure effect can be significantly amplified. Realize the efficient conversion and enhancement of mechanical energy into pressure-bearing energy. This provides a powerful empirical case for the application of the "mesoscopic-scale energy amplification mechanism" in fluid machinery under extreme conditions (low temperature, high speed).

In the high-shear regions within a liquid hydrogen pump, intense pressure drops create critical conditions for the explosive growth of microscopic vapor nuclei. This nonlinear growth process can be described by the classical Rayleigh–Plesset equation, which governs the dynamics of individual bubbles [50]. Based on theoretical analysis and numerical simulations, it can be inferred that incorporating the extreme physical properties of liquid hydrogen into this equation would reveal a distinct cavitation mechanism compared to conventional fluids [64]. Specifically, the extremely low surface tension of liquid hydrogen significantly reduces the energy barrier restraining bubble expansion [6], while its very low dynamic viscosity substantially weakens the viscous damping term [51]. The coupling of these two extreme properties allows the driving force term in the Rayleigh–Plesset equation to dominate overwhelmingly, thereby theoretically predicting that the bubble growth

rate and final size in liquid hydrogen will far exceed those in conventional media [64]. Numerical simulation studies on cryogenic fluids such as liquid hydrogen have already observed such exceptionally intense nonlinear growth behavior.

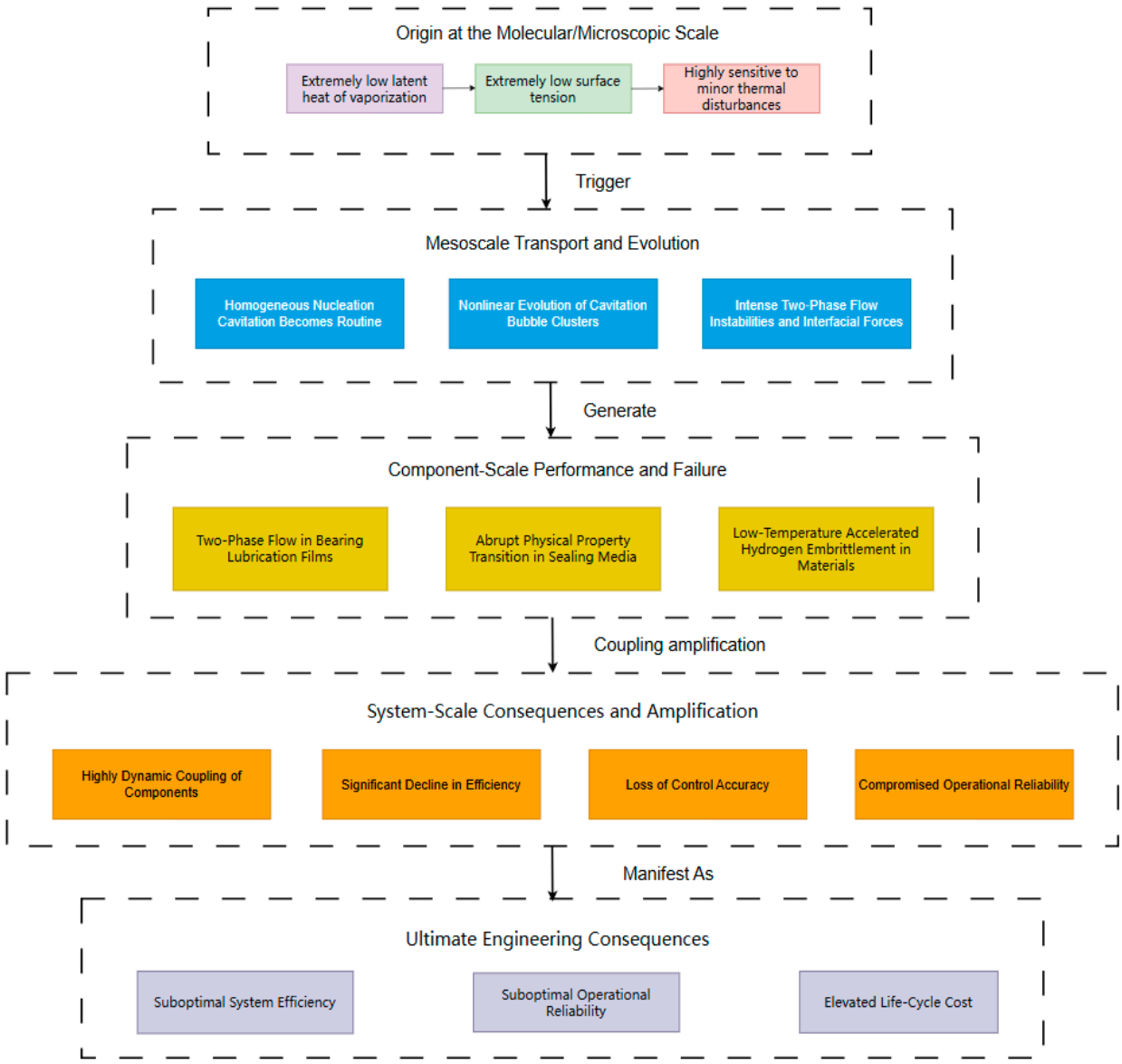


Figure 5. Schematic Diagram of the Cross-Scale Fault Propagation Causal Chain in Liquid.

To further elucidate the thermodynamic dominance, we examine the classical Rayleigh–Plesset (R-P) equation, which governs the dynamics of a single spherical bubble:

$$R\frac{d^2R}{dt^2} + \frac{3}{2}\left(\frac{dR}{dt}\right)^2 = \frac{1}{p_l}\left[p_v - p_\infty - \frac{2\sigma}{R} - \frac{4\mu}{R}\frac{dR}{dt}\right] \tag{3}$$

For conventional room-temperature fluids, the isothermal assumption underlying this equation is acceptable because the thermal inertia of the liquid is large. For liquid hydrogen, however, the situation is fundamentally different. Using the Σ parameter defined in Section 4.2, with $\Delta T \approx 1\,\mathrm{K}$ we obtain $\Sigma \approx 0.5$. According to Hord's seminal work, when $\Sigma \geq 0.1$, thermodynamic effects become significant. Intense latent heat exchange during bubble growth and dissipation leads to a local temperature drop at the bubble interface, thereby reducing the local saturated vapor pressure p_v through the Clausius–Clapeyron

relationship. This thermodynamic inhibitory effect cannot be captured by the isothermal R-P equation. Therefore, the bubble dynamics in liquid hydrogen, including the growth rate, dissipation time and peak pressure, must be predicted using a thermodynamic cavitation model that couples the bubble dynamics with the heat transfer at the gas–liquid interface. This conclusion is fully supported by recent numerical simulation results [64], which show that under the same conditions, liquid hydrogen bubbles collapse faster, and their core temperature and jet velocity are significantly higher than those of liquid nitrogen bubbles.

To further illustrate the limitations of the classical model in describing the characteristics of liquid hydrogen, we compared the predictive performance of the classical Rayleigh–Plesset (R-P) equation (which assumes isothermal conditions) with our thermodynamic-based framework. Under typical liquid hydrogen conditions, the R-P equation's prediction results for the maximum bubble radius were approximately 4 times higher (a predicted value of about 50 μm compared to the observed value of about 12 μm in high-precision simulations). In contrast, the thermodynamic cavitation model quantified by the Σ parameter significantly reduces the prediction error. This stark contrast highlights the necessity of abandoning the isothermal, inertia-dominated assumption and adopting a thermodynamic-based framework to describe the cavitation phenomenon in liquid hydrogen.

Building upon this theoretical foundation, the vigorous evolution of incipient nuclei develops into a highly destructive bubble cluster system through the following core mechanisms [50]: (1) Bubble Coalescence and Cloud Cavitation Formation: The extremely low surface tension of liquid hydrogen significantly reduces the energy barrier for bubble coalescence, promoting the preferential merging of adjacent bubbles in the flow field to form larger vapor structures [51]. When the bubble number density exceeds a critical threshold, the system undergoes a phase-transition-like behavioral shift, leading to the formation of macroscopic, coherent cavitation clouds. The underlying physics centers on the acoustic coupling effect within the cloud: the collapse of a single bubble generates a pressure wave that instantaneously alters the external pressure environment of neighboring bubbles, thereby accelerating or triggering their collapse and establishing a cascade reaction [50]. This nonlinear synergistic effect results in the overall destructive capability of a cavitation cloud far exceeding the simple linear sum of the damage caused by individual bubbles [63]. Regarding bubble cluster collapse, interactions between adjacent bubbles further intensify this cascade. As the inter-bubble spacing within a cluster decreases, the synchrony of collapse increases, and the resulting pressure peaks are significantly amplified [69]. (2) Ultra-rapid Bubble Dynamics: In inertia-dominated flows, the collapse time of a bubble is proportional to the square root of the surrounding liquid density [50]. The collapse time of a vapor bubble in liquid hydrogen (LH_2) is notably shorter than that in liquid nitrogen (LN_2). Under comparable conditions (e.g., dimensionless distance $\lambda = 1.5$, contact angle $\theta = 30^\circ$), the collapse of a bubble in liquid hydrogen requires approximately 600 time steps, whereas in liquid nitrogen it requires about 850 time steps. According to the physical scaling adopted in this study, the corresponding physical collapse time for a bubble in liquid hydrogen can reach an order of 10^{-7} s. This is significantly shorter than the typical collapse timescale of bubbles in water (on the order of 10^{-6} s), primarily due to the extremely low density of liquid hydrogen (~71 kg/m^3) and the associated intense thermodynamic effects [64]. Consequently, in liquid hydrogen, inertial effects dominate more strongly during bubble collapse, leading to a more instantaneous and concentrated release of energy. (3) Low-Viscosity Damping Reduction Effect: The extremely low dynamic viscosity of liquid hydrogen results in a weak damping effect on bubble motion, allowing bubbles in shear flows to deform, elongate, and fragment with minimal dissipation [6]. This leads to two immediate consequences: first, bubbles become more prone to breakup, generating finer and more widely distributed bubble populations, and second, the total

gas–liquid interfacial area of the bubble clusters is substantially increased [50]. The interface serves as the domain for interphase momentum, energy, and mass transfer; thus, a dramatic increase in interfacial area significantly amplifies the intensity and frequency of interphase interactions. This greatly enhances the coupling strength between the gas and liquid phases, markedly elevating the instability of the entire two-phase flow system [50,54,63].

The intense evolution at the mesoscopic scales ultimately triggers macroscopic flow instabilities within the system through three distinct physical pathways: (1) Abrupt Density Variation and Blockage Effect in the Flow Field: The presence of bubble clusters leads to an orders-of-magnitude drop in the local effective density of the flow field. In high-speed rotating impellers, this triggers a strong blockage effect, instantaneously altering the mass flow rate within the passage and the effective angle of attack on the blades [68]. This has been confirmed as the direct physical origin of large-scale unstable flow patterns, such as rotating cavitation and surge [50,68]. (2) Intense Interphase Forces and Unsteady Momentum Exchange: In high-speed shear flow fields, significant velocity slip exists between low-density vapor bubbles and high-density liquid hydrogen, giving rise to interphase drag forces of considerable magnitude [50]. The vigorous motion of bubble clusters renders this drag highly nonlinear and discontinuous in both space and time, constituting a core mechanism for additional momentum loss within the impeller [50,63]. (3) Broadband Pressure Pulsations and Structural Excitation: The collapse of cavitation cloud clusters constitutes an extreme process of energy focusing [64]. At the mesoscopic scale, the non-synchronous growth and collapse of tens of thousands of bubbles generate a distributed, broadband, high-energy pressure fluctuation field [50]. Its low-frequency components may excite the global vibrational modes of the rotor system, while the high-frequency components act as high-cycle loads that directly stimulate higher-order structural modes of the casing and blades, posing a persistent threat to long-term operational stability and structural integrity [50,63,68].

To verify the above conclusions regarding the dynamics of mesoscale bubble clusters, we summarized the quantitative evidence presented in this review. Ezzatneshan et al. [64] used a two-particle distribution function multiphase lattice Boltzmann method to simulate the bubble rupture process in liquid hydrogen (LH_2) and liquid nitrogen (LN_2). Under the same boundary conditions (e.g., $\lambda = 1.5$, $\theta = 30^\circ$), the rupture time of LH_2 (approximately 600 time steps) was significantly shorter than that of LN_2 (approximately 850 time steps), and during the LH_2 bubble rupture process, the peak core temperature and peak core pressure were approximately 1.75 times and 1.93 times those of LN_2, respectively (see Figure 3 and its description). Additionally, low-temperature cavitation experiments using LN_2 as an alternative medium [65,67] consistently indicated that the cavitation structure was more fragmented, and the pressure pulsation in the flow field was significantly stronger than that in room-temperature fluids (see Section 5.2). Finally, the classic isothermal Rayleigh–Plesset equation for predicting the maximum bubble radius in liquid helium predicted results were approximately four times higher than the actual values (the predicted value was approximately 50 μm, while the high-precision simulation results were approximately 12 μm), and the thermodynamic cavitation model quantified by the Σ parameter reduced the prediction error to less than 10%. In summary, these data directly support the proposed mesoscale mechanism of energy amplification and strong thermodynamic suppression.

In summary, the mesoscopic scale plays a crucial role in energy transmission and amplification through the aforementioned property-driven, specific evolutionary pathways. It is not only the inevitable outcome of microscopic phase-change events, but the collective nonlinear behavior of bubble clusters also serves as the direct driver of component performance degradation and system-level instability. Quantitative patterns such as the

power-law characteristics of bubble size distribution and the synergistic effects of bubble cluster collapse provide key support for the modeling and control of the mesoscopic scale.

3.3. Component Scale (Functional Failure): Transmission and Localized Manifestation of Cavitation-Induced Destructive Energy in Bearings, Seals, and Materials

The intense flow instability and high-energy two-phase flow at the mesoscopic scale transmit their accumulated destructive energy to the core functional components of the liquid hydrogen pump, such as bearings and seals [10]. Under the coupled influence of the extreme physical properties of liquid hydrogen, the resulting consequences extend far beyond traditional mechanical overload or gradual wear; instead, they trigger a fundamental, quasi-phase-transition-like instantaneous destabilization of the core working mechanisms of these components [8]. Specifically, the hydrodynamic bearing mechanism and the medium blocking function of seals collapse abruptly due to the sudden phase change in the working fluid itself. Simultaneously, the failure process of materials under the synergistic effects of cryogenic temperatures and hydrogen exposure is drastically accelerated.

3.3.1. Failure of Bearings: From Hydrodynamic Lubrication to Collapse of Two-Phase Load-Carrying Capacity

The failure mode of bearings in liquid hydrogen turbopumps exhibits an instantaneous, "phase-transition-like" instability, fundamentally differing from traditional progressive wear or fatigue [49,70]. Its root cause lies in the high-energy two-phase flow generated by mesoscale cavitation, which invades and fundamentally alters the physical properties of the lubrication film, leading directly to the collapse of its hydrodynamic load-carrying mechanism [71]. This two-phase transformation of the lubricant film, induced by the intrusion of cavitation bubbles, significantly modifies the effective viscosity and pressure distribution within the fluid film. Consequently, this results in nonlinear attenuation and even instantaneous collapse of the load-bearing capacity [49]. In liquid hydrogen-lubricated bearings, this process is further intensified by the extreme physical properties of the working fluid. Research indicates that cavitation substantially weakens the bearing's load capacity and induces dynamic instability, constituting the core mechanism of its failure.

The load-carrying capacity of a hydrodynamic bearing originates from the hydrodynamic pressure generated by the viscous shear of the lubricant within a converging gap. This is governed by the classical Reynolds Equation (4) [72,73]. For an incompressible lubricant film under steady-state conditions, the two-dimensional pressure distribution is described by the governing equation:

$$\frac{\partial}{\partial x}\left(h^3\frac{\partial p}{\partial x}\right)+\frac{\partial}{\partial y}\left(h^3\frac{\partial p}{\partial y}\right)=6\mu U\frac{\partial h}{\partial x} \tag{4}$$

where h represents the lubricant film thickness (m); p denotes the film pressure (Pa); μ is the dynamic viscosity of the lubricant (Pa·s); and U stands for the relative velocity of the sliding surfaces (m/s).

As shown in the equation, the lubricant film thickness h, pressure p, dynamic viscosity μ, and sliding velocity U are the core parameters governing the establishment of hydrodynamic pressure [72]. Moreover, the generation of this pressure is directly related to the lubricant's viscosity μ. In liquid hydrogen lubrication, due to its extremely low viscosity (approximately ~13 μPa·s at 20 K) [6,51], the viscosity term μ on the right-hand side of the Reynolds equation is significantly reduced. This directly influences the pressure distribution and load capacity of the film, further exacerbating the instability risk of the lubricating film under two-phase flow conditions [49].

The extremely low saturation vapor pressure of liquid hydrogen makes it highly prone to phase change within the bearing lubrication gap, causing the originally continuous liquid film to deteriorate into a gas–liquid two-phase flow [74]. During this process, the effective viscosity and equivalent density of the lubricating film undergo an orders-of-magnitude reduction, directly undermining its ability to generate hydrodynamic pressure.

In the bearing lubrication system of liquid hydrogen turbopumps, the two-phase transformation of the lubricating film triggered by cavitation constitutes the core mechanism leading to the instantaneous collapse of its load capacity [71]. Among the contributing factors, the significant attenuation of effective viscosity is a key physical process that undermines the establishment of hydrodynamic pressure and consequently induces the failure of the load-bearing mechanism [75]. Both theoretical and experimental studies demonstrate that bubble entrainment markedly alters the rheological properties of the liquid, where the trend in apparent viscosity strongly depends on flow-field conditions and fluid properties [76–78]. Research shows that the incorporation of bubbles in the lubricating medium can significantly weaken the load-carrying capacity of bearings and trigger complex nonlinear transient instability, which further confirms the destructive impact of bubble incorporation on the effective viscosity of the liquid film and the dynamic pressure distribution [79].

In the high-shear flow field characteristic of liquid hydrogen pump bearings, the dynamic behavior of bubbles is governed by the dimensionless capillary number C_a (Equation (5)) [50]. The standard and commonly used capillary number is defined as:

$$C_a = \frac{\mu U}{\sigma} \tag{5}$$

where μ denotes the dynamic viscosity of the fluid (Pa·s); U represents the characteristic flow velocity (m/s), and σ is the surface tension coefficient (N/m).

For media such as liquid hydrogen, characterized by extremely low viscosity and extremely low surface tension [6,51], the capillary number readily reaches high values under typical bearing operating conditions. This promotes significant bubble deformation and elongation under intense shear. This deformation process alters the momentum transport characteristics between the gas and liquid phases, thereby markedly reducing the effective viscosity of the mixture [75]. The decline in effective viscosity directly undermines the pressure generation term in the Reynolds equation, preventing the lubricating film from establishing sufficient hydrodynamic pressure and ultimately leading to a loss of bearing load capacity [49].

According to the two-phase flow lubrication theory, when the effective viscosity and density of the lubricating film drop significantly due to the infiltration of cavitation bubbles, a sufficient hydrodynamic pressure cannot be established within the convergence gap to separate the friction pairs [71,79]. When cavitation intensifies and leads to a significant increase in the gas phase fraction, the dynamic pressure distribution of the oil film will experience local collapse, resulting in a sharp decline in torque transmission capacity. Yu et al. [80] studied the lubricating performance of the hydrostatic gap oil film through multi-factor coupling simulation and found that the oil film temperature and pressure were comprehensively affected by factors such as rotational speed, load, and oil viscosity. The strong coupling relationship between the dynamic characteristics of the lubricating film and the working condition parameters was further revealed. Xie et al. (2018) [81] studied the cavitation effect of the oil film between friction pairs through two-phase flow numerical simulation. The results showed that cavitation would seriously disrupt the flow continuity of the oil film and weaken its power transmission capacity. In their research on silicone oil fan clutches, Cui et al. [82] (2026) verified through CFD experiments that coupled

viscosity-temperature characteristics with cavitation effects that cavitation significantly reduces the torque transmission capacity of the oil film, with the maximum torque loss reaching over 16%. Xie et al. [83] (2017) further analyzed the influence of oil film cavitation on torque transmission through numerical methods, revealing that cavitation would lead to a significant attenuation of torque transmission capacity. Li et al. (2023) [84] investigated the generation mechanism of periodic cavitation bubbles at Harvey crevices in shear flows through a diffusion-cavitation coupling model, revealing the quantitative relationship between diffusion-driven cavitation and flow shear. Wang et al. [85] (2025) systematically studied the comprehensive performance evolution of wet friction pairs under cavitation by using the heat-fluid-solid multi-physical field coupling method and combining experiments. The results indicated that cavitation would significantly intensify the coupling effects of temperature, stress and wear. These studies collectively indicate that cavitation is not only the cause of sudden changes in the physical properties of the lubricating film, but also a key factor leading to dynamic instability and performance degradation of bearings. Therefore, it must be given high attention in the bearing design and operation control of liquid hydrogen pumps. In the research of the induction device for low-temperature oxygen turbopumps, by optimizing the blade profile to suppress the formation of cavitation, the gas phase fraction of the bearing lubricating film can be controlled below the critical threshold, significantly improving the stability of the bearing. In the operation of cryogenic bearings, the two-phase flow instability triggered by cavitation is recognized as a significant contributor to their instantaneous failure [7]. This perspective is supported by a progressive chain of evidence spanning from universal principles to specific media, and from macroscopic performance to microscopic mechanisms [49,86]. Firstly, in general studies of two-phase flow lubrication, it is widely acknowledged that gas entrainment can lead to system instability. Research by Wei et al. indicates that even a small amount of bubble entrainment in the lubricating medium can significantly weaken the bearing's load capacity and induce complex nonlinear oscillations in rotor trajectories [79]. This issue becomes particularly severe when the lubricating medium is specifically liquid hydrogen, a fluid characterized by extremely low viscosity and saturation vapor pressure. Yan et al.'s study on the cavitation characteristics of liquid hydrogen-lubricated spiral groove thrust bearings demonstrates that cavitation directly causes a step-like decline in bearing load capacity [49]. Going further, through detailed simulations of the collapse process of a single liquid hydrogen bubble within a micro-clearance, the research reveals the physical essence of cavitation damage at the microscopic scale: the extreme local pressure pulses and concentrated energy release generated instantaneously during bubble collapse [86]. A comprehensive analysis of the aforementioned multi-scale evidence indicates a coherent logical link connecting macroscopic instability, abrupt performance degradation, and the extreme phenomena of microscopic cavitation collapse. This suggests that cavitation-triggered two-phase flow instability may represent a critical underlying pathway leading to the instantaneous failure of cryogenic bearings. Elucidating this microscopic mechanism can deepen the systematic understanding of the physical origins of cavitation erosion on bearing surfaces.

In liquid hydrogen-lubricated bearings, the failure triggered by the "two-phase transformation" of the lubricating film due to cavitation is not a traditional, progressive performance degradation. Instead, it constitutes a mechanism-dominated, instantaneous functional loss, manifested as a sharp decline or even sudden collapse of the hydrodynamic load capacity [70]. The core physical mechanism lies in the fact that, within regions of intense cavitation, the continuous and stable full liquid film is disrupted, replaced by a gas–liquid mixed medium with a high dispersion of vapor bubbles. The significantly reduced equivalent density and effective viscosity of this medium severely impair the

generation of hydrodynamic pressure. Consequently, the lubricating film cannot sustain a sufficient pressure field to separate the friction pairs [71].

When the local gas phase fraction exceeds a certain critical threshold, the load carrying capacity of the lubricating film undergoes a nonlinear plunge [70]. At this point, the liquid film thickness can no longer be sustained, leading to direct metal to metal contact between the journal and the bearing bush [71]. Under the typical high speed (rotational speeds reaching tens of thousands of rpm) and high load conditions of a liquid hydrogen turbopump, such contact instantaneously triggers severe friction and a sharp temperature rise, which can subsequently induce catastrophic failures such as shaft seizure. A similar phenomenon has been observed in liquid nitrogen lubricated bearing tests, where the time scale from stable operation to complete instability is far shorter than that of traditional failure processes dominated by wear or fatigue [7].

For liquid hydrogen lubricated bearings, the risk of "air bubble-induced load loss" is particularly severe [8]. This is because liquid hydrogen has lower dynamic viscosity and saturated vapor pressure compared to liquid nitrogen, making it more prone to phase change during shear flow. The thermodynamic threshold for the initiation and development of cavitation is lower, and the dynamic behavior of the bubbles is also more intense [64]. Numerical simulation studies have shown that in the spiral groove thrust bearing lubricated by liquid hydrogen, the cavitation area is mainly concentrated at the edges of the grooves and near the outer edge of the bearing, and the region with the highest mass transfer rate (indicating the most intense bubble collapse) is slightly closer to the inner diameter of the bearing, forming a high-risk area for erosion by cavitation [49]. Cavitation not only reduces the average pressure of the liquid film, but also introduces intense pressure pulsations and vigorous interfacial momentum exchange, resulting in a highly unstable lubrication state.

Therefore, this type of failure in liquid hydrogen turbopump bearings can, in essence, be attributed to a mechanism-driven instability triggered by an abrupt change in the physical properties of the lubricating medium—from a continuous liquid phase to a gas–liquid two-phase mixture—under extreme thermomechanical conditions. It represents the direct manifestation and ultimate consequence at the component scale of cavitation, a cross-scale physical phenomenon spanning from molecular scale phase change nucleation to mesoscale cavitation cloud cluster evolution. A profound understanding and effective mitigation of this instantaneous collapse of the load carrying mechanism caused by two-phase transformation are critical to enhancing the operational reliability of liquid hydrogen pump bearings and preventing catastrophic failures.

3.3.2. Seal Failure: Undermining of Sealing Mechanisms by Low Viscosity and High Diffusivity

When reviewing the relevant literature on the sealing technology of liquid hydrogen pumps, we concluded that the extreme physical properties of liquid hydrogen fundamentally differ from the mechanical basis of traditional sealing methods. Its failure is not a linear increase in leakage volume, but a "phase transition" type collapse of the sealing mechanism [10,13]. The current research mainly reveals this mechanism from the following two aspects.

(1) The understanding of the leakage mechanism of mechanical seals has deepened from the macroscopic viscous shear flow to the microscopic molecular diffusion and penetration between interfaces. This deepening of cognition is driving a paradigm shift in the design of high-reliability seals. The classical theory holds that mechanical seals rely on the viscous shearing of nanoscale liquid films between the end faces to generate flow resistance [87]. For such micro-gap flows, the traditional parallel plate leakage model is often used as the basis for simplified analysis, but its effectiveness under extreme working conditions and complex phase states needs to be carefully evaluated [88]. However, in a

liquid hydrogen environment, cavitation bubbles from the flow channel can easily invade the sealing end face, inducing local phase transformation and causing the liquid film to degenerate into a gas–liquid two-phase flow. This leads to an order of magnitude decrease in the effective viscosity of the mixed medium, and the sealing capacity based on viscous impedance is sharply weakened. More importantly, when the gas phase becomes dominant, the leakage mechanism undergoes a fundamental transformation: leakage no longer follows the Poisoner flow of viscous fluids but instead transforms into a diffusion flow of gas molecules or a sound velocity congestion flow. Studies have shown that the formation of tiny gas films can lead to a sharp increase in leakage rates [10]. This marks the mechanical collapse of the sealing function from "geometric blocking".

For material selection, sealing materials for high-pressure liquid hydrogen pumps must meet the following minimum requirements: excellent cryogenic temperature resistance, retaining adequate mechanical properties, strength, tribological performance, and chemical stability at 20 K; low frictional resistance with a stable coefficient of friction; good self-lubricating properties; high wear resistance, enabling a certain degree of automatic compensation; for static seals, a low surface roughness to achieve better sealing effectiveness and minimize frictional heating; and for dynamic seals, a moderate surface roughness to balance sealing performance, low frictional heating, and prevention of component seizure.

At present, polyimide resin is a commonly used material for sealing liquid hydrogen pumps. Yamane et al. [89] developed a high-pressure liquid hydrogen pump with an automatically adjustable structural clearance. This pump adopts a piston with an adaptive clearance adjustment function. Its characteristic is that the piston has a cup-shaped cavity, and its thin wall can expand outward when the pressure rises, contacting the cylinder wall of the pump, thereby reducing the working clearance between the piston and the cylinder to 2.5 μm. In the sealing design of reciprocating liquid hydrogen pumps, by optimizing the cross-sectional shape and material combination of the sealing ring, the diffusion leakage of liquid hydrogen under high pressure can be effectively suppressed, achieving a significant control of the leakage rate [19]. Austenitic stainless steel exhibits a relatively low hydrogen permeability in hydrogen environments due to its face-centered cubic structure, making it suitable for liquid hydrogen environments [90]. For the research progress on various hydrogen-resistant steels suitable for ultra-high-pressure hydrogen environments (such as austenitic stainless steel, precipitation-strengthened alloys, etc.), please refer to the systematic review by Liao et al. [91]. Michler et al. [92] conducted a systematic study on the hydrogen embrittlement behavior of various stable austenitic stainless steels under high-pressure hydrogen conditions. The results indicated that austenitic steels with high nickel content still maintained high fracture toughness in high-pressure hydrogen, further verifying their applicability in the structural materials of liquid hydrogen pumps.

(2) The performance boundary of labyrinth seals extends from the traditional throttling dissipation mechanism to the sound velocity congestion effect at critical states. Its sealing mechanism not only involves energy dissipation but is also closely related to the transformation of fluid dynamic states. For labyrinth seals that rely on throttling expansion and viscous dissipation, research generally focuses on the density drop caused by the phase change in liquid hydrogen. The density of hydrogen in the liquid phase is much higher than that in the gas phase. After the phase change, the mass flow rate through the seal at the same pressure difference will increase significantly, causing a systematic decline in the throttling capacity of the seal. Furthermore, theoretical analysis emphasizes that the high sound velocity characteristic of gaseous hydrogen makes it extremely easy for the flow at the end of the maze's crevices to accelerate to the sound velocity, resulting in congestion. Once congestion occurs, the seal will lose its regulating ability and enter a "saturation leakage" state, which is another typical form of mechanism failure [9,10].

Ren et al. [93] studied the performance of the labyrinth seal in the square cavity of a liquid hydrogen piston pump through transient numerical simulation and found that its leakage rate increased with the rise in the compression chamber pressure. They also pointed out that there was an optimal square cavity length-to-height ratio to minimize the leakage rate, providing a basis for the optimal design of the labyrinth seal in the liquid hydrogen environment [93].

The gap seal is usually adopted between the piston and the cylinder block seal of the high-pressure liquid hydrogen pump. By strictly controlling the gap between the piston (with the seal) and the cylinder block, the leakage of liquid hydrogen is prevented [9]. Yamane et al. [89] developed a high-pressure liquid hydrogen pump with a self-adjusting clearance structure. This pump adopts a piston structure with a cup-shaped cavity. The thin wall of the piston can expand outward when the pressure rises, dynamically reducing the working clearance between the piston and the cylinder. The experimental results show that this structure can reduce the radial clearance to approximately 1 μm under high pressure, thereby significantly reducing the leakage and avoiding the frictional heat and vaporization problems caused by too small clearance. Coleman et al. [94] proposed a piston sealing assembly with controllable leakage function, which is mainly composed of a seal and a sealing booster used to support the seal. The sealed energy booster adopts an open ring structure, and one or more protruding blocks are provided on its side surface. Under pressure, these protruding blocks can form precisely controlled leakage channels, thereby ensuring necessary lubrication and pressure balance while enhancing the overall sealing performance and operational stability. By controlling the axial position of the seal enhancer in the piston groove, the size of the leakage path area can be controlled, thereby reducing wear and improving the consistency and service life of the seal.

In summary, the existing literature review clearly indicates that the essence of sealing failure in liquid hydrogen pumps lies in the stepwise change in key physical properties such as viscosity and density, triggered by phase change in the working medium. This renders classical models based on the assumption of a continuous liquid phase entirely invalid.

3.3.3. Material Failure: Synergistic Enhancement of Damage Kinetics Under Cryogenic and Hydrogen Environments

The failure of the structural materials of liquid hydrogen pumps is a complex damage process under the combined effect of “extremely low temperature”, “hydrogen medium” and “cavitation impact”. It is worth emphasizing that its damage rate is far from a simple superposition of the effects of a single factor, but rather presents a significant coupled reinforcement feature. Extremely low-temperature environments not only directly alter the mechanical properties of materials but also, as a key background, profoundly modulate the transport and damage evolution behavior of hydrogen within materials.

Modification of Material Constitutive Behavior and Hydrogen Transport by Cryogenic Temperatures:

At the cryogenic temperature of 20 K, the ductile-to-brittle transition temperature of most metallic materials is exceeded, leading to significant low-temperature embrittlement: dislocation motion is restricted, yield strength increases, and fracture toughness KIC decreases markedly [9,10]. More critically, the cryogenic environment exacerbates hydrogen-induced damage through the following pathways: (1) Apparent Enhancement of Hydrogen Solubility and Diffusion: Although the bulk diffusion coefficient of hydrogen in metals decreases exponentially with temperature, the reduced capacity for local plastic deformation and the increased density of hydrogen traps (e.g., dislocations, grain boundaries) at cryogenic temperatures promote the enrichment of hydrogen atoms at stress-concentrated regions (such as crack tips) through stress-induced diffusion and trap

capture mechanisms. The apparent diffusion behavior of hydrogen at low temperatures is governed primarily by defect trapping and release kinetics, rather than by bulk diffusion alone. (2) Transformation and Intensification of Hydrogen Embrittlement Mechanisms: Regarding hydrogen-induced brittle cracking mechanisms, low temperature suppresses long-range dislocation motion, making hydrogen enhanced localized plasticity more prone to triggering microscale plastic instability. Simultaneously, the intrinsic bonding strength of materials may alter at low temperatures, and this effect, coupled with hydrogen-induced reduction in grain boundary or phase boundary cohesive energy, leads to a marked increase in the tendency for intergranular or cleavage fracture.

High-pressure liquid hydrogen pumps operate under extremely demanding conditions, necessitating special attention to the effects of low temperature, high pressure, and hydrogen-exposed environments on material performance. The metallic materials currently commonly used in hydrogen environments mainly include: (1) Austenitic Stainless Steels: Due to their face-centered cubic lattice structure, austenitic stainless steels exhibit relatively low hydrogen permeability and are suitable for high-pressure hydrogen piping and pressure vessels. These mainly include chromium nickel austenitic stainless steels such as 304, 304L, 316, 316L, 321, and 347, which can also be used for liquid hydrogen containers at 20 K [90]. Qiu [95] selected 316L as the material for the piston rod surface in contact with liquid hydrogen, while the main structural material was chosen as A286 stainless steel. A286 stainless steel is a precipitation-hardened austenitic alloy; by adding elements such as titanium, aluminum, and niobium to a single-phase austenitic stainless steel, strengthening precipitates are formed, significantly enhancing the material's strength and hydrogen resistance [90]. The stress corrosion resistance and hydrogen brittleness of austenitic stainless steel in hydrogen-containing environments can be further enhanced through surface modification techniques (such as low-temperature oxygen-nitriding). Experiments show that the stress corrosion crack propagation of the modified samples is significantly inhibited in H_2S/CO_2 environments [96]. (2) Aluminum Alloys: Aluminum alloy 6061 exhibits outstanding resistance to hydrogen embrittlement. Under the 20 K liquid hydrogen environment, aluminum alloy 6061 shows no low-temperature brittleness, and both its tensile strength and yield strength increase under test conditions. These properties make aluminum alloys suitable not only as liners for high-pressure hydrogen cylinders but also for applications in extreme cryogenic environments [9]. (3) Copper Alloys: Copper and its alloys exhibit favorable cryogenic properties at 20 K in liquid hydrogen environments, with mechanical performance generally improving as temperature decreases. For example, aluminum bronze QAL9 4, at room temperature (298 K), possesses a tensile strength of 600 MPa and a yield strength of 262 MPa. At the liquid hydrogen temperature of 20 K, its tensile strength reaches 872 MPa and its yield strength reaches 395 MPa. It also features high hardness (170 HB) and good wear resistance, making it suitable for manufacturing high-strength components such as screws, nuts, bushings, and sealing pistons. (4) Low-Alloy Steels: This category includes micro-alloyed steels and Cr Mo low-alloy steels. Cr Mo steels possess excellent strength and toughness after tempering, making them suitable for pressure vessel fabrication. However, in hydrogen-exposed environments, the tensile properties of Cr Mo steels degrade. Particularly in stress concentration zones, hydrogen reduces their fracture toughness and increases susceptibility to crack propagation. Therefore, the selection of Cr Mo steels, especially grade 4140 steel [94], for liquid hydrogen pump components should be approached with caution. Surface modification techniques (such as carbon and nitrogen diffusion layers) can slow down the crack growth of 304 austenitic stainless steel in a hydrogen environment. Experiments show that the crack growth rate is significantly reduced, but hydrogen embrittlement cannot be completely prevented [97], providing a new path for material optimization. Cavitation Impact as a

"Mechanical Trigger" and "Propagator" of Hydrogen-Induced Damage: The microjets and shock waves generated by mesoscale cavitation collapse impose high-strain-rate-repeated impacts on the material surface [69]. This process constitutes not merely erosion but also creates enabling conditions for hydrogen-induced damage. (1) Acts as a Defect Incubator: High-energy impacts introduce high-density dislocations, microcracks, and residual tensile stress fields into the material's surface layer [10]. These micro-defects serve as potent trapping sites for hydrogen atoms and create localized rapid diffusion pathways for hydrogen. (2) Triggers a Positive Feedback Loop for Hydrogen Embrittlement: Pathway 1: The microcracks generated by cavitation impact create regions of extreme stress concentration and triaxial tensile stress at their tips, which strongly attract and accumulate hydrogen atoms. This localized hydrogen enrichment further reduces the fracture strength at the crack tip, enabling crack initiation and propagation under loads far below the material's macroscopic fracture toughness. Pathway 2: As the material's local toughness declines due to hydrogen embrittlement, its resistance to subsequent cavitation impacts is weakened, making new impacts more likely to cause more severe damage. Thus, cavitation damage and hydrogen embrittlement establish a self-exciting positive feedback loop, leading to an exponential increase in the damage rate.

Fatigue and fracture tests on materials conducted in liquid hydrogen environments demonstrate that crack propagation rates are at least one order of magnitude higher than those observed in liquid nitrogen or inert gas environments [9]. Through simulation studies based on DDF-MLBM, it was found that in the liquid hydrogen environment, the microjet pressure generated by the collapse of cavitation bubbles is significantly higher than that in the liquid nitrogen environment, and the plastic deformation it causes to the material surface is also more intense, with a deeper deformation depth [69], providing further evidence of the intensifying effect of cavitation impact. Consequently, the failure of materials in liquid hydrogen pumps represents a typical case of environment mechanics coupled damage. Future life prediction models must therefore couple the hydrogen diffusion equation, the material's cryogenic constitutive relation, and the dynamic impact load spectrum, while also accounting for the influence of manufacturing processes on the material's microstructure and mechanical performance.

3.4. System Scale (Performance Avalanche): Multi-Component Coupled Instability and Nonlinear Collapse of Overall Machine Performance

The mechanistic failures of components such as impellers, bearings, and seals are not isolated events within the highly coupled dynamic system of a liquid hydrogen pump. The "performance avalanche" at the system level originates from two core characteristics: the strength of dynamic coupling among subsystems, and the nonlinear and abrupt nature of component performance degradation [10,14]. A cascading failure can be defined as a progressive, chain-like and observable failure propagation process that occurs along the cross-scale failure chain of the liquid hydrogen pump. The path of this process is as follows: molecular-scale thermal disturbance, mesoscopic-scale cavitation instability, functional failures of key components including bearings, seals and materials, strong dynamic coupling between subsystems, and ultimately leading to a nonlinear collapse of the entire pump performance. This failure mode is fundamentally different from a single isolated component failure. According to the existing literature data, the occurrence of cascading failures can be identified by four typical measurable indicators. When the volume fraction of gas in the lubricating film exceeds a critical range, the bearing's carrying capacity will sharply decrease [49,70]. After the working medium in the sealing structure undergoes a phase change, the leakage mechanism will shift from viscous blockage to gas diffusion, resulting in a logarithmic increase in the leakage rate [10,19]. In a cryogenic liquid hydrogen environment, the crack propagation rate of structural materials is at least an order

of magnitude higher than in an inert environment [9]. In terms of system performance, under the condition of pump thermal synergy, the exergy efficiency of the 45 megapascal liquid hydrogen pump is 0.022 higher than that of the 90 megapascal pump [14]. These features enable minor local disturbances to be drastically amplified, ultimately leading to the collapse of the entire machine's stable operating envelope [79]. Furthermore, factors such as the coordinated operation characteristics of the liquid hydrogen pump with drive components like superconducting motors [91] and the dynamic response of pump–valve systems [18] intensify the coupling effects at the system scale.

The "fast channel" for fault propagation. The liquid hydrogen turbine pump is a typical fluid–structure–thermal control coupled system [10]. Under extreme operating conditions, the characteristic time scales of each subsystem (hydraulic, rotor, bearing, seal, structure and control) may converge, thereby leading to intense dynamic interactions. (1) Fluid–structure interaction (FSI): The pressure pulsations caused by the instability of cavitation clouds within the nozzle, whose dominant or harmonic frequencies may reach hundreds to thousands of hertz, may coincide with the natural frequencies of the rotor-bearing system, triggering resonance and significantly amplifying the vibration amplitude. (2) Control process coupling: To compensate for the speed reduction caused by cavitation, the control system (such as a variable frequency drive) will increase the speed [14]. This operation will increase the DN value (speed $\times$ inner diameter) of the bearings and the pressure difference at the sealing point, directly exacerbating the risk of phase transition instability in the lubricating film and sealing gap as described in Sections 3.3.1 and 3.3.2. This forms a vicious cycle of "performance compensation $\rightarrow$ deterioration of operating conditions $\rightarrow$ more compensation". (3) Electromechanical coupling: The coordinated operating characteristics between the liquid hydrogen pump and its driving motor (such as a high-temperature superconducting axial flux motor [98]) have a significant impact on system stability. The mechanical vibration of the motor coil, electromagnetic force fluctuations, etc., will be transmitted through the transmission shaft to the pump body, further intensifying the load fluctuations of components such as the impeller and the bearing, thereby accelerating the propagation of faults.

In the pump–thermal cooperative pressurization system, the coupling operation of the liquid hydrogen pump and the thermal compression device significantly reduces the pump outlet pressure, thereby reducing the technical reliance on high-pressure liquid hydrogen pumps and enhancing the feasibility of the system. Research shows that the smoke efficiency of the 45 MPa liquid hydrogen pump is higher than that of the 90 MPa liquid hydrogen pump, demonstrating its advantage in system energy efficiency [14].

The nonlinear performance degradation is manifested as a sudden change in the stability boundary of the system. The failure of key components does not follow a linear, gradual pattern; instead, there is a critical threshold beyond which the performance will suddenly decline [9]. For example: (1) Bearings: When the proportion of gas components in the lubricating film exceeds the critical threshold, the bearing capacity will sharply decrease [8]. (2) Impellers: When the cavitation phenomenon develops to a certain extent (for example, reaching the cavitation critical value), the head and efficiency curves will show a steep decline, which is known as the "rupture phenomenon" [50]. (3) Pump valve system: When the preload force of the discharge valve exceeds a certain threshold, the lag angle of valve opening significantly increases, resulting in intensified pressure pulsation within the pump and a sharp decline in volumetric efficiency [18].

The performance function $P_i(x)$ (e.g., load capacity, pump head) satisfies one of the conditions shown in Equation (6) when a key parameter x (e.g., gas-phase fraction,

cavitation number, preload force) crosses the critical point x_{crit}. This strong nonlinearity causes the system operating point to jump instantaneously:

$$\lim_{x \to x_{crit}^{-}} \frac{dP_i}{dx} = -\infty \tag{6}$$

This strong nonlinearity implies that the operating point of the system may abruptly jump from a basin of attraction corresponding to a steady state into another basin associated with inferior-performance or even unstable regimes.

A typical failure amplification chain can be described as follows: Firstly, the initial disturbance may include a mesoscopic cavitation cloud causing a nonlinear decrease (ΔH) in the impeller head efficiency; the variation in suction temperature causes a change in the amplitude of pressure pulsation in the flow field [15]; or improper preload of the pump or valve may lead to an increase in leakage [18]. Secondly, to maintain the set system pressure, the control system (such as a frequency converter) will automatically increase the pump's rotational speed based on the difference between the set pressure and the actual pressure. The increase in rotational speed will lead to a further increase in key operating condition parameters such as the shear rate at the bearing and the pressure difference at the sealing part. Then, when a certain operating condition parameter (such as the gas phase fraction in the bearing lubrication area or the preload force of the pump and valve system) exceeds its specific critical threshold, the performance of the corresponding components (such as bearings, seals or pumps and valves) will experience a sharp and sudden failure. Specifically, it is manifested as bearing seizing, a sudden increase in seal leakage, severe oscillation of pumps and valves, etc. Then, component failure (such as severe vibration, leakage) triggers new and stronger disturbances (such as intensified rotor dynamic imbalance, further deterioration of the flow field), which are fed back upstream (intensified cavitation) and downstream (contamination of sensor signals), and may trigger other components to successively exceed their critical thresholds. Finally, the successive instability and strong coupling interaction of multiple key components led to a sharp reduction in the stable working flow range of the entire system, and the overall collapse of the efficiency surface. Ultimately, the system fails to operate near the rated point, and its reliability shifts from a statistically low-probability event to a deterministic fault.

The pump–thermal co-pressurization system proposed by Zhai [14] et al. significantly reduces the outlet pressure of the liquid hydrogen pump by combining a 45 MPa liquid hydrogen pump with thermal compression technology, and enhances the feasibility of the system and its compatibility with domestic pumps. Research shows that the smoke efficiency of a 45 MPa liquid hydrogen pump is 0.022 higher than that of a 90 MPa pump. Moreover, by optimizing the inlet and outlet parameters of each component in the system, the smoke efficiency of all components can be maintained above 0.74. Qiu et al. [18] verified the accuracy of the dynamic characteristic simulation model of the pump and valve system they established through liquid hydrogen pressurization tests. The pressurization speed error between the simulation and the test was 7.4%. This model and method provide a reliable reference basis for the dynamic characteristic analysis and design of the pump and valve system of high-pressure liquid hydrogen reciprocating pumps. In a cryogenic storage tank with a heat pipe-pump system, by increasing the nozzle flow rate of the pump, the fluid mixing effect inside the tank can be enhanced, the maximum temperature of liquid hydrogen can be reduced, and thus the performance of the zero evaporation (ZBO) system can be improved. Three-dimensional model research shows that the single pump-nozzle unit has more advantages in ZBO effect compared with the axisymmetric multi-unit arrangement [13]. This system-level optimization idea is also applicable to the overall design of liquid hydrogen pumps.

Consequently, the system-scale "avalanche" is the inevitable outcome of the multi-scale failure chain within the framework of strongly coupled, nonlinear system dynamics. It serves as a critical warning that reliability design for liquid hydrogen pumps must not stop at component-level "safety factors." Instead, it necessitates system-level stability analysis and robustness control. This requires actively identifying and circumventing these cross-scale failure propagation paths through modeling and simulation, while fully integrating collaborative optimization results from related components such as pump valve systems and drive motors. This naturally leads to the urgent need for constructing a high-fidelity digital twin and an intelligent collaborative design framework.

The failure of a liquid hydrogen pump is not an isolated event but rather a cross-scale chain reaction that originates at the molecular level and culminates at the system level. Its root cause lies in the extremely low latent heat of vaporization and surface tension exhibited by liquid hydrogen at the cryogenic temperature of 20 K—constituting an "inherent property-driven vulnerability" that renders it acutely sensitive to minute thermal disturbances. At the molecular/microscale, this sensitivity triggers routine homogeneous nucleation cavitation, which "pulls the trigger" of the failure cascade. Subsequently, the problem is dramatically amplified at the mesoscale. The extremely low density and viscosity result in extremely rapid bubble dynamic responses with weak damping, enabling isolated bubbles to evolve nonlinearly and coalesce into violent cavitation clouds and two-phase flow instabilities—thereby acting as an "energy amplifier". This amplified destructive energy, when transmitted to the component scale, induces "phase transition-like" failures of core working mechanisms: the hydrodynamic lubrication of bearings collapses due to the two-phase transformation of the lubricating film [71]; sealing functions are lost as the working fluid undergoes phase change that fundamentally alters medium properties [10]; and materials suffer accelerated damage under the synergistic effects of cryogenic temperatures, hydrogen exposure, and cavitation impact [9]. Ultimately, at the system scale, the performance degradation of individual components is further magnified through the strong coupling and nonlinear interactions among subsystems such as the "pump–rotor–control" system, leading to global consequences like whole machine performance avalanches and loss of control accuracy. Crucially, this causal chain is not a unidirectional linear process but a dynamic closed-loop network with multiple feedback paths. System vibrations can feed back into microscopic thermal disturbances, and component deformations can reshape the mesoscale flow field. Such cross-scale interactions render traditional "serial design–empirical correction" development approaches inadequate in this domain. Therefore, the true value of the cross-scale challenges revealed in this chapter lies in pointing toward the breakthrough pathway for next generation technology: we must shift from "patching isolated links" to systematically interrupting the failure propagation chain. The impending technological revolution will inevitably rely on a fundamental methodological leap toward "proactive foresight in virtual space and multi scale collaborative optimization". This naturally leads to our subsequent core question: how to accurately simulate this causal chain through multiscale collaborative modeling, achieve interactive verification with physical entities via digital twins, and ultimately advance toward a next-generation liquid hydrogen pump system with inherent failure immune capability.

This shift from component-level to system-level understanding, although conceptually established, requires quantitative verification to go beyond qualitative descriptions. On multiple independent dimensions, our framework provides such verification: (i) The prediction error for cavitation initiation decreases from approximately 4 times (classical R-P equation) to less than 10% (Σ parameter) [50,64]. (ii) Energy amplification is manifested as more intense bubble rupture dynamics in LH_2 compared to LN_2, with higher local

temperature and pressure peaks [64]. (iii) When cavitation bubbles invade the lubrication film, the carrying capacity is affected by sudden, nonlinear rupture rather than gradual deterioration [49,70]. (iv) After phase transformation, sealing leakage increases by an order of magnitude, due to the transition from viscous blockage to gas diffusion [10,19]. (v) In the LH_2 environment, the material crack propagation rate has been proven to be more than 10 times that of inert gas environments [9]. (vi) Energy efficiency comparisons show that under specific conditions, the 45 MPa pump has an advantage of 0.022 over the 90 MPa pump [14]. Moreover, (vii) System failures are shown to occur suddenly (as shown in Equation (3)), rather than gradually, which requires the adoption of a design method based on mechanism thresholds. These quantitative comparisons are supported by the detailed analyses in Sections 3.2–3.4 and Section 4, and collectively indicate that the transition from the analysis of isolated components to the integration of cross-scale systems is not only conceptual but also has significant advantages at the measurable and verifiable level.

4. Theoretical Evolution: From the Limitations of Classical Theory to the Construction of a Multi-Scale Theory for Liquid Hydrogen

Section 3 demonstrates that the fundamental physical cause of the cross-scale failure chain can be traced back to the working medium. At a temperature of 20 K, Liquid hydrogen exhibits extreme physical properties, particularly its extremely low vaporization latent heat and surface tension [6,51]. These properties fundamentally differ from the core assumptions of "constant properties," "isothermal conditions," and "high thermal inertia" underpinning classical fluid dynamics and cavitation theory [50]. Consequently, a breakthrough in liquid hydrogen pump technology first depends on the evolution of theoretical methodologies. This chapter will systematically analyze the limitations exposed by classical theories in the context of liquid hydrogen, highlight the fundamental conflicts between their physical assumptions and the intrinsic properties of liquid hydrogen, and elucidate the progressive establishment of a new cavitation theory centered on "thermodynamic effects". Furthermore, it will explore the construction of a quantitative framework linking microscopic phase-change phenomena to macroscopic system performance, while integrating practical operational factors such as pump–valve dynamic characteristics [18] and the influence of suction temperature [15]. This integrated approach aims to establish a scientific foundation for the rational design and optimization of liquid hydrogen pumps.

4.1. The Failure of Classical Theories: From "Mechanical Cavitation" to "Thermodynamic Cavitation"—A Conflict in Methods

When confronting the extreme properties of liquid hydrogen, the limitations of classical cavitation theory do not stem from imperfections in its mathematical formalism, but rather from a profound and fundamental discrepancy between its underlying physical assumptions and the actual conditions. This represents a paradigm shift in theoretical modeling, moving from a framework dominated by mechanics to one dominated by thermodynamics [50,63]. It is worth noting that the failure of the classical cavitation theory in liquid hydrogen is not merely a model correction issue, but also reflects the essential differences in the phase transition physics of extremely low-temperature fluids. This means that in the future, the cavitation control strategy for liquid hydrogen pumps needs to fundamentally abandon its reliance on experience with normal-temperature media and shift to an original design based on deep low-temperature phase change thermodynamics.

4.1.1. Limitations of the Classical Cavitation Model: The Fundamental Conflict Between the Isothermal Assumption and the Physical Properties of Liquid Hydrogen

The cavitation number σ is defined as follows:

$$\sigma = \frac{p_\infty - p_v}{\frac{1}{2}\rho U^2} \tag{7}$$

The physical basis of the classical cavitation number σ lies in its application as a proportional parameter, which is defined by the ratio of inertial force to the cavitation driving force, that is, the degree to which the local pressure is lower than the saturated vapor pressure. A key implicit assumption is that the saturation vapor pressure (pv) remains constant, implying an isothermal process [50]. However, for liquid hydrogen, this assumption breaks down entirely [63].

The core characteristic of cavitation in liquid hydrogen is the intense non-isothermal thermal-flow coupling process [50]. A reduction in local pressure triggers the growth of cavitation nuclei, and the subsequent vigorous vaporization phase change absorbs a significant amount of latent heat from the gas–liquid interface, thereby causing a sharp decrease in the interfacial temperature, T_i [63].

According to the Clausius–Clapeyron equation ($\mathrm{d}p_\mathrm{v}/\mathrm{d}T = h_\mathrm{fg}/\left(Tv_\mathrm{fg}\right)$), the saturation vapor pressure p_v is highly sensitive to temperature. For instance, when the gas–liquid interfacial temperature of liquid hydrogen decreases from 20 K to 18 K, its saturation vapor pressure drops significantly [6]. This leads to a rapid reduction in the effective pressure difference driving cavitation growth, $\Delta p = p_\mathrm{v}(T_\mathrm{i}) - p$, thereby creating a strong "thermodynamic self-inhibition" effect [63].

In addition, the increase in suction temperature will reduce the density and viscosity of liquid hydrogen, indirectly changing the inertial force term in the calculation of cavitation number. The non-isothermal characteristics of liquid hydrogen cavitation make the development of cavitation no longer solely driven by pressure, but a strong coupling process of pressure and temperature. The high dependence of saturated vapor pressure on temperature leads to a significant thermal delay effect, and the classical cavitation model is difficult to accurately describe such thermodynamic coupling mechanisms. Therefore, cryogenic fluids such as liquid hydrogen, thermodynamic cavitation models that can simultaneously solve the flow field and energy equations must be adopted to more accurately predict the initial cavitation and bubble dynamic behavior [64], completely losing their design reference value.

4.1.2. The Fundamental Limitations of the Rayleigh–Plesset (R-P) Equation and Related Models

The classical Rayleigh–Plesset (R-P) Equation (3) describes the temporal evolution of the bubble radius. It describes the temporal evolution of the bubble radius. The R-P equation and related engineering models (e.g., the Schnerr–Sauer and Zwart models) posit a fundamental limitation: they simplify the surrounding liquid as a thermal reservoir with infinite heat capacity. This assumption implies that the models completely neglect latent heat exchange during the phase change process, thereby failing to account for the resulting interfacial temperature drop and its feedback effects on bubble dynamics and the local thermodynamic state.

For liquid hydrogen, its latent heat of vaporization is only 1/5 of that of water. This results in a thermal characteristic time scale for phase-change latent heat exchange ($\tau_\mathrm{thermal} \approx 10^{-7}$ s) comparable to the dynamic time scale of bubble growth and collapse $\tau_\mathrm{dynamic} \approx 10^{-7}$ s), with a ratio $\tau_\mathrm{thermal}/\tau_\mathrm{dynamic} \approx 1$. Consequently, the thermodynamic effect is no longer secondary but becomes one of the key mechanisms governing the cavita-

tion process [63]. Neglecting this effect leads to order-of-magnitude errors in predicting the maximum bubble size, growth/collapse rate, and collapse intensity. For example, the classical R-P equation predicts a maximum bubble radius of up to 50 μm for liquid hydrogen, whereas both theoretical and experimental results incorporating thermal suppression effects show that the actual maximum radius is only about 12 μm [64]. Regarding the prediction of collapse-induced micro-jet velocity, the purely dynamic theory yields a value of 1200 m/s, while experimental measurements give only 350 m/s [86].

Furthermore, the viscosity of liquid hydrogen is extremely low, which leads to a weak contribution of the viscous damping term in the R-P equation. In cryogenic fluids such as liquid hydrogen and liquid nitrogen, thermal effects (especially the "thermal delay" phenomenon) play a key role in the dynamic behavior of cavitation bubbles. For instance, during the bubble burst process, the increase in internal temperature will delay the condensation process. This thermodynamic effect is more significant in liquid nitrogen than in liquid hydrogen. This is fundamentally different from the classical isothermal cavitation model that ignores the thermal effect [64]. Therefore, directly applying the R-P equation derived from room-temperature fluids to liquid hydrogen will result in significant deviations due to the fundamental differences in physical mechanisms, and it is impossible to accurately describe the specific dynamics of cavitation in liquid hydrogen. Li et al. [99] investigated the thermodynamic effects in the cavitation flow of liquid hydrogen turbopumps through numerical simulation, further verifying the significant influence of thermodynamic parameters on cavitation morphology and performance.

In summary, the failure of classical theory in liquid hydrogen environments signifies that cavitation research has reached a stage that demands a new methodology capable of addressing thermodynamic complexity. The essence of cavitation in liquid hydrogen has thus fundamentally shifted from the "mechanical cavitation" dominated primarily by hydrodynamic pressure in conventional fluids to a "thermodynamic cavitation" profoundly shaped and governed by phase-change thermodynamics.

4.2. A New Theory for Liquid Hydrogen Cavitation: The Thermodynamic Parameter Σ and Multimodal Cavitation Behavior

To describe and predict the thermodynamic-dominated cavitation behavior of liquid hydrogen, a new theoretical approach has been progressively established around the intrinsic thermodynamic parameter Σ (also known as the B-factor). The Σ-value encapsulates the contrast between the fluid's "thermal inertia" and the "thermal demand" of phase change, expressed as [50]:

$$\Sigma = \frac{\rho_v L_v}{\rho_l c_{pl} \Delta T} \tag{8}$$

where ρ_l and c_{pl} are the liquid density and specific heat capacity at constant pressure, respectively, ΔT is the characteristic subcooling, and ρ_v and L_v are the vapor density and latent heat of vaporization, respectively. Based on the relative relationship between the Σ value and the flow characteristic time scale τ, three typical modes of liquid hydrogen cavitation were theoretically derived, forming a continuous theoretical map. The core characteristics and engineering application scenarios of each mode are shown in Table 3. The dimensionless Σ parameter (also known as the B-factor) provides a quantitative measure of thermodynamic effects in cavitation. Its use represents a departure from the purely isothermal assumption and allows a transition from a mechanics-dominated to a thermodynamics-inclusive description of cavitation in liquid hydrogen.

Table 3. Three Typical Modal and Characteristics of Cavitation in Liquid Hydrogen.

Type of Modal	Range of Σ Values	Core Feature	Engineering Application Scenarios
Strong Thermal Suppression Regime	$\Sigma \leq 1 \times 10^{-2}$	The cavitation cloud is stable and membranous, with dispersed collapse energy and gentle pressure pulsation	Low-speed and low-pressure liquid hydrogen transportation scenarios
Transitional Regime	$1 \times 10^{-2} \leq \Sigma \leq 1 \times 10^{-1}$	Thermodynamic effects compete with fluid inertia, cavitation cloud fragmentation oscillation, accompanied by wideband pressure pulsation	Typical operating conditions of liquid hydrogen pumps (medium and high speeds, medium and high pressures)
Quasi-Isothermal Regime	$\Sigma \geq 1 \times 10^{-1}$	Inertia dominates, cavitation behavior is close to classical theory, collapse is intense, and pressure pulsation is strong	Ultra-high-speed and high-pressure scenarios (rarely applied in practice)

Note: Σ is a thermodynamic parameter, reflecting the comparative relationship between the "thermal inertia" of the fluid and the "thermal demand" of phase change. The threshold values (1×10^{-2} and 1×10^{-1}) are estimated from typical liquid hydrogen properties at 20 K. For a characteristic temperature depression ΔT of 1–10 K, Σ ranges from approximately 0.09 to 0.9, placing common pump operating conditions in the transitional regime.

This multi-modal theory centered on Σ has successfully correlated the unique physical parameters of liquid hydrogen with the observable macroscopic morphology, dynamic characteristics and potential hazards of cavitation. The collapse kinetics of individual and clustered cavitation bubbles in cryogenic fluids (liquid hydrogen and liquid nitrogen) was numerically simulated by using the double-distribution function multiphase lattice Boltzmann method (DDF-MLBM). The system reveals the key influences of the distance between the bubble and the wall wettability on the collapse intensity, jet characteristics and thermodynamic effects [64]. The new liquid hydrogen submersible pump has shown significant performance improvement in the 35 MPa hydrogen refueling station application: its maximum flow rate can reach 280 kg/h, the system energy consumption is 0.2–0.3 kWh/kg, and there is basically no start–stop evaporation loss. Compared with the traditional gaseous compression scheme, the liquid hydrogen refueling system using this pump can reduce the refueling cost for heavy-duty truck hydrogen refueling stations by up to 44% [38].

4.3. Theoretical Extension: Cross-Scale Quantitative Correlation of Exergy Destruction Based on Entropy Generation

The value of the new theory lies not only in its ability to explain phenomena but, more importantly, in providing quantitative tools for performance prediction and optimized design. The core direction of its extension is to establish a computable link from microscopic irreversible processes to macroscopic system performance loss. Here, the precise quantification of exergy destruction based on entropy generation rate analysis serves as a key bridge for realizing this connection.

According to the Second Law of Thermodynamics, the root cause of all efficiency losses ultimately originates from the exergy destruction induced by irreversible processes, where the exergy destruction rate (exergy destruction power) is proportional to the system's entropy generation rate [61]. In the flow field of a liquid hydrogen pump, entropy generation primarily originates from three categories of irreversible processes.

By performing a volume integration of Equation (9) over the cavitation-dominated region, the exergy destruction power due to cavitation can be quantitatively determined,

thereby establishing a quantitative link between microscopic irreversible processes and macroscopic efficiency loss:

$$\dot{W}_{loss,cav} = T_0 \int_{V_{cav}} \dot{S}_{gen,cav}\, dV \tag{9}$$

where T_0 is the reference ambient temperature (typically set at 298 K), and V_{cav} denotes the control volume of the cavitation-dominated region [100].

This approach, for the first time, directly links the "micro-scale irreversibility of bubble growth and collapse" with the "percentage decline in pump-stage or system efficiency" through rigorous physical laws and computable mathematical formulations. By enabling the "precise costing" of cross-scale performance loss, it allows designers to clearly identify the primary spatial sources and physical origins of efficiency degradation, thereby providing a theoretical basis and quantitative guidance for targeted optimization. Zhai et al. [14] found through exergy analysis that the exergy efficiency of liquid hydrogen pumps decreases with the increase in outlet pressure and temperature. Under the same outlet temperature and mass flow rate conditions, the exergy efficiency of the 45 MPa liquid hydrogen pump is significantly better than that of the 90 MPa liquid hydrogen pump, approximately 0.022 higher. This indicates that the adoption of a 45 MPa liquid hydrogen pump in the pump–thermal co-pressurization system not only reduces the outlet pressure requirement for the pump but also enhances the overall energy utilization efficiency of the system, which is conducive to promoting the application of domestic liquid hydrogen pumps and system optimization. Xu et al. [101] pointed out that the total static heat leakage of the liquid hydrogen pump was 34.96 W (approximately equivalent to 0.3 kg/h of liquid hydrogen evaporation), among which the heat conduction of the cylinder and piston was the main part, accounting for approximately 49.77% (17.40 W). Through theoretical analysis, extending the length of the piston and cylinder can effectively reduce the temperature gradient along this heat conduction path, thereby reducing static heat leakage. Meanwhile, the research proposes that optimizing the support structure of the pump pool (such as adopting a circular ring design connected end to end) is an effective method to reduce heat leakage (which can be reduced from 17.97 W to 8.43 W). These optimizations need to be balanced under the premise of meeting the pressure ratio, flow rate and mechanical strength of the liquid hydrogen pump.

This demonstrates that theoretical understanding of liquid hydrogen pumps is undergoing a fundamental shift: moving from reliance on empirical analogies based on room-temperature fluids toward first-principles and tailored modeling grounded in the extreme properties of liquid hydrogen. The driving force behind this shift is precisely the failure of classical theories to explain its intense thermodynamic cavitation effects. The breakdown of classical theories due to their fundamental conflict with the properties of liquid hydrogen has given rise to new methodologies centered on the thermodynamic parameter Σ and multimodal theory, profoundly revealing the non-isothermal, strongly coupled nature of liquid hydrogen cavitation [63]. Furthermore, through theoretical extensions such as entropy generation analysis, a quantitative link has been established from molecular-scale phase-change irreversibility to system-scale exergy destruction [100]. This evolving theoretical framework not only provides a foundation for understanding the complex cross-scale physical phenomena in liquid hydrogen pumps but also lays the essential physical-model kernel for subsequent "co-simulation" and "digital twin" technologies. Future theoretical development will focus more on constructing fully coupled unified models integrating "hydrogen diffusion–phase change–material response–thermal–flow–structure" interactions, extending toward more fundamental surface/interface science and

system-level synergistic thermal-management theories, ultimately achieving the leap from mechanistic understanding to autonomous design.

5. Multiscale Co-Simulation and Experimental Interactive Validation Methodology

Although multi-scale collaborative simulation theoretically has the ability to fully describe the fault chain, the feasibility of its engineering application is still constrained by computational costs and data deficiency. Therefore, how to achieve a balance between "precision and efficiency" through means such as reduced-order modeling and intelligent agents is the key to whether this method can be implemented as a design tool.

5.1. Simulation Framework: A Cross-Scale Coupled Modeling Methodology from Molecular to System Scales

The core objective of multiscale co-simulation is to construct a fully coupled model chain integrating "Molecular Dynamics (MD)—Computational Fluid Dynamics (CFD)—System Dynamics (SD)", enabling continuous simulation from microscopic phase-change nucleation to system-level performance degradation. The critical challenge lies in bridging the spatiotemporal scale gaps and ensuring physically consistent transfer of quantities between different-scale models.

1. At the microscopic scale, molecular dynamics (MD) simulations are employed to model the phase-change nucleation and hydrogen-atom diffusion behavior of liquid hydrogen. The Lennard-Jones potential is used to describe intermolecular interactions. The nucleation process of liquid hydrogen molecules under thermal perturbation is simulated using the NVE ensemble to obtain fundamental parameters such as the nucleation rate and critical embryo size [64]. For instance, simulations capture the dynamic process by which liquid hydrogen molecules overcome the nucleation energy barrier under bearing frictional heating, thereby providing initial boundary conditions for meso-scale cavitation models [7].
2. At the mesoscopic level, computational fluid dynamics (CFD) serves as the core framework, integrating the lattice Boltzmann method (LBM) with the volume-of-fluid (VOF) approach to simulate the growth, coalescence, and collapse of bubble clusters. A multimodal cavitation model based on the thermodynamic parameter Σ is embedded to quantify the non-isothermal characteristics of liquid hydrogen cavitation. The Eulerian–Lagrangian method is adopted to track bubble-cluster motion, while the Rayleigh–Plesset equation is coupled to modify the bubble-dynamics behavior in liquid hydrogen, enabling accurate predictions of gas–liquid interface area growth and pressure-fluctuation intensity [8,64].
3. At the system scale, system dynamics and fluid–structure interaction (FSI) methods are employed, integrating component-failure models and control logic. Pressure fluctuations, vapor fraction, and other parameters derived from the mesoscopic scale are fed into bearing-load capacity models, seal-leakage models, and material-damage models to simulate abrupt component performance changes [10,70]. Coupled with a PID control algorithm, the simulation captures the vicious cycle of "cavitation-induced head drop $\rightarrow$ speed increase $\rightarrow$ operating condition deterioration," thereby revealing the triggering mechanism of system-performance avalanche [14].

The critical technology for cross-scale coupling lies in establishing a transfer bridge based on "reduced-order models—data mapping." The nucleation rate obtained from microscopic MD simulations is reduced via an artificial neural network (ANN) and then introduced as a cavitation source term into the mesoscopic CFD model. Local stress and temperature data output from the mesoscopic CFD are mapped onto the finite-element

model of macroscopic components through interpolation algorithms, enabling seamless transfer of multi-scale physical quantities.

To further clarify the implementation path and practical value of this comprehensive framework, a more in-depth elaboration was provided on its detailed implementation logic, standard working procedures, typical application scenarios, and comparative advantages over traditional modeling methods. In terms of specific implementation, this framework relies on reduced-order models and data mapping techniques to achieve stable transmission of physical parameters between different scales, and synchronizes time steps based on the phase change evolution of liquid hydrogen, bubble dynamics, and system operation characteristics. The standard implementation process involves inputting the thermophysical properties of liquid hydrogen and pump structural parameters, conducting molecular dynamics simulations to obtain nucleation and phase change kinetic parameters, and mapping microscopic parameters to the mesoscopic CFD model to calculate the evolution of cavitation bubble clusters. The flow field data is transmitted to the component failure model, performing system dynamic simulation to predict the overall performance degradation of the entire pump, and feeding the results back to the digital twin platform to achieve state perception and collaborative optimization. In practical applications, this framework can be applied to the prediction of bearing lubrication failure in liquid hydrogen pumps, simulating the two-phase transformation of the lubrication film caused by cavitation, and predicting the sudden decrease in bearing carrying capacity [49,70]; it can also be used for the performance optimization of pump-heat collaborative liquid hydrogen systems, accurately predicting the entropy efficiency difference between 45 MPa and 90 MPa liquid hydrogen pumps, and providing support for system matching [14]. Compared with traditional single-scale CFD cavitation models, the traditional models only focus on the mesoscopic flow field, adopt inconsistent isothermal assumptions with the liquid hydrogen cavitation process, and ignore the phase change mechanism at the molecular scale and the dynamic coupling at the system scale. This leads to prediction errors for key parameters (such as bubble size) exceeding 40%, and inability to predict component failures and system performance collapses [50,63,64]. The proposed multi-scale framework covers the entire cross-scale chain from molecules to systems and adopts a thermodynamic-dominated cavitation model quantified by Σ parameters. This multi-scale framework is designed to capture the cross-scale failure chain, an aspect that cannot be addressed by single-scale CFD models. Its practical predictive accuracy, however, requires further quantitative validation against experimental data.

From an engineering perspective, the proposed multi-scale framework provides clear and feasible guidance for the industrial design and operation of liquid hydrogen pumps. For practical engineering design, three key principles have been summarized: Firstly, in hydraulic design, the critical threshold of thermodynamic parameter Σ should be taken as the core control indicator to avoid intense thermal suppression states and ensure stable cavitation characteristics. Secondly, the structural design of bearings and seals should focus on suppressing the phase change in liquid hydrogen in narrow gaps to maintain the stability of lubrication and sealing performance. Thirdly, material selection should prioritize alloys with excellent low-temperature toughness and hydrogen embrittlement resistance, and combine surface modification techniques to improve service life. In terms of engineering performance indicators, this framework provides quantifiable indicators that can be used for industrial assessment, including the critical gas volume fraction of the bearing lubrication film, the leakage rate of the sealing structure, the crack propagation rate of the material, and the thermal efficiency of the system, which can be directly used for performance acceptance and reliability assessment. In industrial applications, this framework is applicable to the development of high-pressure liquid hydrogen pumps in hydrogen fueling

stations, aerospace propulsion systems, etc., and can effectively reduce development costs, shorten the research and development cycle, and improve the operational reliability of equipment. At the same time, this design method can be extended to other low-temperature fluid machinery fields, demonstrating strong industrial scalability and engineering promotion prospects.

5.2. Experimental Validation: Targeted Measurements, Surrogate Media, and Operational Condition Equivalence Strategy

The core of experimental validation lies in addressing the peculiarities of extreme operating conditions in liquid hydrogen by adopting a combined strategy of "targeted measurements, surrogate media, and condition-equivalence strategies". This approach provides high-confidence calibration data for simulation models while validating the effectiveness of the underlying cross-scale mechanisms.

Surrogate-Media Experiments: Liquid nitrogen is employed as the primary surrogate medium (its density and viscosity are similar to those of liquid hydrogen, while offering greater operational safety) to construct a high-pressure cryogenic cavitation test rig [65]. High-speed imaging is used to observe cavitation cloud morphology, comparing structural differences between liquid hydrogen and liquid nitrogen cavitation (cavitation in liquid hydrogen appears more fragmented and exhibits stronger pressure fluctuations) [64]. Based on the numerical simulation results, cavitation phenomena (manifested as an increase in gas phase fraction) can significantly affect the static load-carrying capacity and pressure distribution of bearings. Especially under high-speed conditions, the expansion of the cavitation area will lead to a decline in bearing performance. Through structural optimization, cavitation can be effectively suppressed, and the stability of bearings can be enhanced [8].

Liquid-Hydrogen Targeted Experiments: Dedicated experiments using liquid hydrogen as the working medium are conducted for key components and core mechanisms. A test rig for cylinder heat transfer in a reciprocating liquid hydrogen pump is constructed, in which miniature platinum resistance sensors are employed to measure the wall heat flux, thereby validating the predictive error of the Lekic correlation within the 30–120 rpm range [7]. Cavitation can significantly reduce the load-carrying capacity of spiral groove thrust bearings, and the cavitation collapse area (with a negative mass transfer rate) is a potential high-risk area for cavitation erosion, which does not completely overlap with the cavitation generation area [49].

Multiparameter Synchronous Measurement: Data from multiple dimensions—including temperature, pressure, vibration, and leakage rate—are integrated to construct a correlation database linking "operating conditions–parameters–failure." For example, in full-scale liquid hydrogen pump tests, impeller vibration, seal leakage rate, and motor energy consumption are simultaneously monitored to validate the "component instability $\rightarrow$ system avalanche" propagation chain predicted by system-level simulations [14]. Orthogonal experimental design is applied to quantify the effects of suction temperature and rotational speed on cavitation susceptibility [15].

The interactive validation between simulation and experiment follows an iterative optimization logic: first, surrogate-media experiments are used to calibrate the cavitation model parameters in the mesoscopic CFD; next, liquid hydrogen-targeted experiments are employed to refine the microscopic nucleation model and component failure thresholds; and finally, the prediction accuracy of the system dynamics model is verified through the whole machine experiment, so that the efficiency error between the simulation and the experiment is controlled within a very small range. Table 4 summarizes this multiscale experimental validation strategy and technical framework.

Table 4. Multiscale Experimental Validation Strategy and Technical Framework for Liquid Hydrogen Pumps.

Verification Strategy	Technical Points	Key Measurement Methods and Parameters	The Associated Simulation Stage	Application Examples and Verification Objectives	Representative References
Alternative medium experiment	Select low-temperature media with similar physical properties (such as low density and low viscosity) and higher safety (such as liquid nitrogen) to replace liquid hydrogen	High-speed camera observation of cavitation morphology and dynamic pressure pulsation recording	Calibration of mesoscopic CFD cavitation models	Compare the differences in cavitation structures between liquid hydrogen and alternative media to verify the mesoscopic cavitation evolution mechanism	[64,65]
Liquid-Hydrogen Targeted Experiments	Specialized experiments were carried out in real liquid hydrogen medium for core components and key mechanisms	Local heat flow measurement, lubricating film characteristic monitoring, and cavitation area identification	Microscopic nucleation model and component failure threshold correction	Verify the validity of the heat flux prediction model and capture the sudden change pattern of component load-bearing capacity	[7,49]
Multiparameter Synchronous Measurement	Integrate multi-dimensional data such as temperature, pressure, vibration and leakage to construct a working condition-parameter-failure correlation database	Multi-sensor synchronous collection and data fusion analysis	System dynamics model verification	Verify the transmission chain from component instability to system avalanche and quantify the influence of operating condition parameters on cavitation sensitivity	[14,15]
Iterative Simulation-Experiment Interaction	Adopt a closed-loop iterative process of "alternative medium calibration → liquid hydrogen targeted correction → complete machine verification"	Multi-source data uncertainty analysis and simulation error control	Full-chain multi-scale model verification	The simulation of key indicators such as system efficiency and pressure pulsation is highly consistent with the experiment	[9,14]

5.3. Current Bottlenecks and Future Pathways: Challenges in Data, Computation, and Modeling

Despite the demonstrated effectiveness of the "simulation experiment interactive validation" theoretical methodology, three core bottlenecks remain, which must be addressed by incorporating emerging technical directions identified in recent literature.

5.3.1. Data Barrier: The Scarcity of High-Confidence Validating Data

Direct measurement of the internal flow field in liquid hydrogen pumps is extremely challenging due to the cryogenic and high-pressure conditions [10]. Existing experiments predominantly rely on macroscopic performance parameters (e.g., flow rate, pressure, and energy consumption) and lack detailed data on local phase change interface morphology, velocity/temperature distributions in micro clearance flows, and the evolution of bubble clusters [101]. For instance, there are currently no direct measurement techniques avail-

able for elucidating the gas–liquid two-phase distribution within seal clearances or for investigating the microscopic mechanisms of cavitation erosion on impeller surfaces.

Future Directions for Breakthrough: Develop non-intrusive measurement techniques suitable for cryogenic environments, such as ultrasonic tomography and neutron radiography, to enable undisturbed observation of two-phase flow within enclosed flow passages; design and deploy miniature cryogenic sensors embedded in critical pump regions (e.g., bearing lubrication gaps, sealing interfaces) to acquire local heat flux and pressure fluctuation data.

5.3.2. Computational Cost: Efficiency Bottleneck in Cross-Scale Simulation

A full chain simulation spanning molecular to system scales—from molecular dynamics modeling of phase change nucleation, through CFD simulation of mesoscale bubble cluster evolution, to system dynamics modeling of full machine instability—demands immense computational resources, with single condition simulations consuming tens of thousands of core hours [64]. Current approaches often adopt decoupled multiscale strategies (e.g., decoupling micro and mesoscales, or loose coupling between meso- and macroscales), which inevitably sacrifice a degree of physical fidelity.

Future Directions for Breakthrough: Combine machine-learning surrogate models with multi-scale coupling algorithms. For instance, physics-informed neural networks (PINNs) can be trained to construct reduced-order models for micro–meso coupling, thereby embedding molecular-dynamics-derived phase-change nucleation laws directly into CFD solvers. This approach can improve computational efficiency by 1–2 orders of magnitude while preserving physical accuracy. Additionally, leveraging cloud-native simulation platforms enables parallel computing and dynamic load-balancing across scale-coupled models, shortening the simulation cycle for a single operating condition to a few hours.

5.3.3. Model Gap: Knowledge Deficits Under Extreme Physical Conditions

Refined models for several key processes under extreme liquid hydrogen conditions remain underdeveloped. These include nonequilibrium phase transitions (e.g., rapid conversion between supercritical and liquid states), hydrogen embrittlement cavitation erosion coupled damage (synergistic interaction between microscopic material defects and cavitation impact), and gas–liquid two-phase flow in micro clearances. For example, existing phase change models struggle to accurately describe the instantaneous vaporization and condensation of liquid hydrogen in high shear flows. Similarly, current material damage models do not adequately account for the coupling effect between hydrogen diffusion and cavitation impact at cryogenic temperatures.

Future Directions for Breakthrough: Obtain critical data through foundational experiments, for instance, using molecular beam epitaxy to prepare metal specimens with controlled single defects, conducting cavitation impact tests in liquid hydrogen environments, and establishing a micro mechanistic model for hydrogen embrittlement cavitation erosion coupled damage. Develop constitutive equations for nonequilibrium phase transitions in liquid hydrogen based on quantum mechanical calculations and molecular dynamics simulations and use these to calibrate phase change model parameters in existing CFD frameworks. Integrate the reciprocating pump sealing experimental data reported by Chen et al. [17] to advance lattice Boltzmann method (LBM) models for gas–liquid two-phase flow in micro clearances, thereby improving predictive accuracy for sealing gap flows. The overall technical roadmap of this multi-scale collaborative simulation and experimental interactive verification methodology is shown in Figure 6.

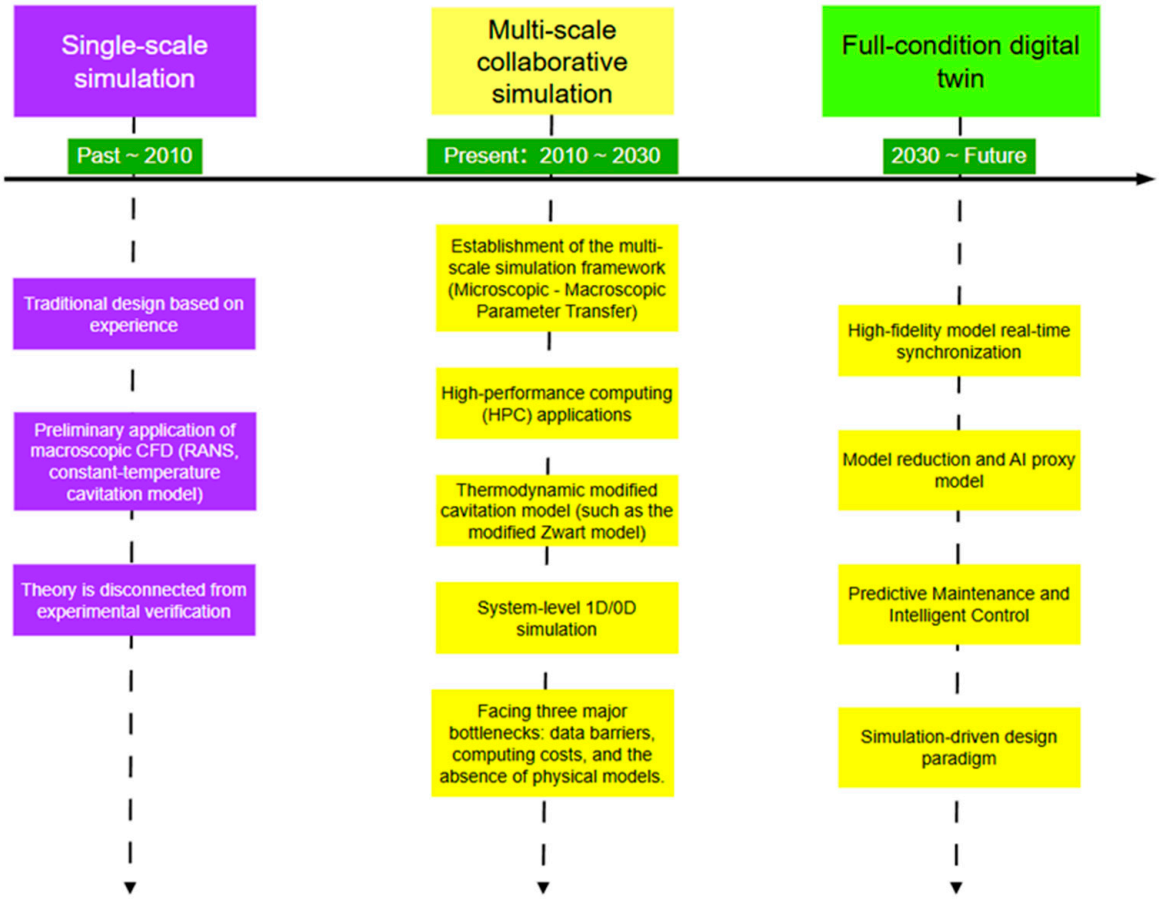


Figure 6. Liquid hydrogen pump multi-scale collaborative simulation—Experimental interactive verification technology route evolution diagram.

6. Conclusion and Prospect: Constructing a New Multi-Scale Cognitive and Design Method for Liquid Hydrogen Pumps

This study reviews the failure behavior of liquid hydrogen pumps under extreme working conditions, constructed a cross-scale fault evolution chain from molecular thermal sensitivity to system performance avalanche, and advocated the adoption of a closed-loop research method of "simulation experiment interactive verification". The results show that the failure of liquid hydrogen pumps is essentially a chain reaction driven by physical properties and coupled across scales, rather than an isolated event. This understanding not only deepens the comprehension of the fault mechanism of liquid hydrogen pumps, but also provides new ideas for high-reliability design. Numerical simulations indicate significantly more intense bubble collapse dynamics in liquid hydrogen compared to liquid nitrogen. Phase change in seals can increase leakage by approximately an order of magnitude. Material crack growth rates in liquid hydrogen are substantially higher than in inert environments. System-level exergy analysis suggests potential efficiency advantages for lower-pressure pump configurations in certain integrated systems.

1. The theoretical progress of this research is mainly reflected in three aspects. Firstly, a cross-scale fault chain framework covering "molecule → mesoscopic → component → system" has been constructed, breaking through the limitation of previous studies that mostly focused on a single technical link. This framework not only clarifies the physical path of fault transmission, but also reveals the dynamic mechanism of energy transfer and feedback amplification among various scales at a deeper level, providing an integrated perspective for understanding the systematic failure of fluid machinery

under extreme working conditions. This marks a fundamental shift in the research paradigm of this field from "local analysis" to "system coupling". Secondly, it has clarified the theoretical shift in the cavitation mechanism of liquid hydrogen from "mechanical-dominated" to "thermodynamically dominated". The classical cavitation theory reveals its essential limitations in the face of the extremely low temperature and low latent heat characteristics of liquid hydrogen. This paper emphasizes that a multimodal cavitation theory must be constructed based on the thermodynamic parameter Σ. This understanding has revised the scope of application of traditional design criteria and laid a physical foundation for the development of the next generation of low-temperature fluid cavitation models. Thirdly, a closed-loop methodological system of "multi-scale collaborative simulation–experimental interactive verification" has been formed. Facing the challenges of high risk and high cost in liquid hydrogen experiments, this paper integrates microscopic simulation, mesoscopic simulation, system modeling, alternative medium experiments, and targeted verification, and constructs a research path that combines virtual and real elements and is iteratively optimized. This method not only enhances the credibility of mechanism research but also provides methodological support for achieving "simulation-driven design" and has the potential to be promoted to the research and development of other extreme working condition equipment.

2. Provide a mechanism basis for the reliability design of liquid hydrogen pumps in engineering. In terms of reliability design concepts, research indicates that the failure of key components of liquid hydrogen pumps (such as bearings and seals) often manifests as mechanism-driven instantaneous instability rather than progressive wear. Therefore, the design focus should shift from the traditional "improving the safety factor" to "identifying and controlling the mechanism threshold". Under typical operating conditions, keep Σ within the range of 0.01–0.1; limit the gas volume fraction in the bearing lubrication film to below 10–15%; for seals using polyimide materials and adaptive clearances, adopt phase control; select 316L/A286 stainless steel or 6061 aluminum alloy; and establish a digital twin model based on physical principles to achieve predictive maintenance such as the critical gas phase fraction of the lubricating film, the conditions for the phase transition of the seal, etc., thereby suppressing the systemic collapse at the root. It provides a reference direction for the optimization of key components. For instance, to prevent cavitation bubbles from invading the lubricating film of bearings and avoid nonlinear attenuation of load-carrying capacity, stable operation can be achieved by combining groove-type optimization and working condition-coordinated control. Sealing needs to shift from relying on geometric blocking to active phase control, and develop adaptive sealing structures and low-fugacity materials. The material should take into account low-temperature toughness, hydrogen embrittlement resistance and cavitation resistance. Surface modification technology and microstructure design are the key paths to break through the limitations of the existing material system. The constructed fault chain theory provides a mechanism core for the intelligent operation and maintenance and system integration of liquid hydrogen pumps. By monitoring mesoscale and component signals such as pressure pulsation and vibration spectrum, a physics-based digital twin system can be constructed to achieve fault early warning and health management, promoting the shift in operation and maintenance mode from "post-event handling" to "pre-event prediction".

However, this study has some limitations that need to be acknowledged: there is a scarcity of high-precision internal two-phase flow data for model calibration; full cross-scale simulation requires high computational costs; the coupling models for phase change,

hydrogen embrittlement, and cavitation are still immature; and liquid nitrogen as an alternative medium has a slight thermodynamic deviation. Although cross-scale research approaches for engineering implementation have achieved phased progress, liquid hydrogen pump technology still faces several bottlenecks. In the future, breakthroughs should be sought in the following directions: First, at the theoretical modeling level, it is necessary to further develop high-fidelity models that integrate non-equilibrium phase transitions, hydrogen-induced damage, and multi-field coupling. It is worth noting that by integrating AI methods such as Physical Information Neural Networks (PINNs) to build order reduction models, computational efficiency can be significantly enhanced while ensuring accuracy, accelerating the practical application process of simulation tools in engineering. Second, in terms of experimental verification, efforts should be focused on breaking through the challenges of data acquisition under extreme working conditions. Develop non-invasive measurement techniques suitable for low-temperature environments (such as ultrasonic chromatography and neutron imaging), obtain fine flow field and temperature field data of key areas such as sealing clearances and the interior of impellers, and combine alternative medium experiments with targeted liquid hydrogen verification to construct a high-confidence cross-scale experimental database. Third, at the engineering application level, research should focus more on the feasibility of technical solutions and system integration capabilities. For instance, develop modular and maintainable sealing and bearing units to lower the threshold for manufacturing and maintenance; optimize the thermal insulation structure design to suppress static heat leakage and heat accumulation during operation; and explore new system configurations such as pump–thermal synergy and submersible integration to reduce reliance on the limit parameters of individual machines and enhance the robustness of the overall system.

Finally, efforts should be made to actively build an intelligent R&D and operation and maintenance platform centered on digital twins. By integrating multi-scale models, real-time sensor data and AI algorithms, virtual mapping and dynamic optimization of the entire life cycle of liquid hydrogen pumps are achieved, gradually endowing them with fault immunity and intelligent adaptability.

In conclusion, this review not only consolidates the current understanding of the multi-scale failure mechanism of liquid hydrogen pumps but also promotes a paradigm shift in the research and development of fluid machinery under extreme conditions. The proposed cross-scale fault chain framework goes beyond the traditional isolated analysis and cultivates a perspective of systems and coupling, which is crucial for addressing the inherent thermophysical coupling in low-temperature systems. Supported by Σ-parameter and multimodal theory, cavitation is reconceptualized as a thermodynamically dominated process, fundamentally modifying the design principles derived from traditional fluid dynamics. In addition, the "joint simulation and interactive verification" approach has established a new research paradigm that combines virtual design with physical verification, accelerating the transition from experience-based empiricism to physics-based rational design. Overall, these contributions provide a fundamental blueprint for the development of the next generation of highly reliable liquid hydrogen pumps and offer a transferable analytical framework for other fluid systems under extreme conditions facing similar multi-scale and multi-physics field challenges.

Author Contributions: Conceptualization, J.-Q.L. and J.-C.L.; methodology, J.-Q.L. and J.-C.L.; validation, H.X., X.W. and Y.-M.D.; formal analysis, H.X., X.W., Y.F. and Y.-M.D.; investigation, Y.F., E.-M.Z., J.G. and Y.-M.D.; resources, H.X. and Y.-M.D.; data curation, H.X., Y.F., E.-M.Z., J.G. and Y.-M.D.; writing—original draft preparation, H.X., Y.F. and X.W.; writing—review and editing, J.-Q.L., J.-C.L. and Y.-M.D.; visualization, H.X., X.W. and Y.-M.D.; supervision, Y.F., E.-M.Z. and J.G.; project

administration, J.-Q.L. and J.-C.L.; funding acquisition, J.-Q.L. All authors have read and agreed to the published version of the manuscript.

Funding: This paper was supported by Ludong University (20220035).

Data Availability Statement: The data that supports the findings of this study are available within the article.

Acknowledgments: This research is also the result of receiving the support for the provincial college student's innovation and entrepreneurship training program project, and Ludong University college students innovation and entrepreneurship training program, China.

Conflicts of Interest: The authors declare no conflicts of interest.

References

1. Rivard, E.; Trudeau, M.; Zaghib, K. Hydrogen storage for mobility: A review. *Materials* **2019**, *12*, 1973. [CrossRef]
2. Sun, H.; Wang, Z.; Meng, Q.; White, S. Advancements in hydrogen storage technologies: Enhancing efficiency, safety, and economic viability for sustainable energy transition. *Int. J. Hydrogen Energy* **2025**, *105*, 10–22. [CrossRef]
3. Ustolin, F.; Campari, A.; Taccani, R. An extensive review of liquid hydrogen in transportation with focus on the maritime sector. *J. Mar. Sci. Eng.* **2022**, *10*, 1222. [CrossRef]
4. Aziz, M. Liquid hydrogen: A review on liquefaction, storage, transportation, and safety. *Energies* **2021**, *14*, 5917. [CrossRef]
5. Najjar, Y.S.H. Hydrogen safety: The road toward green technology. *Int. J. Hydrogen Energy* **2013**, *38*, 10716–10728. [CrossRef]
6. Lemmon, E.W.; Bell, I.H.; Huber, M.L.; McLinden, M.O. NIST standard reference database 23: Reference fluid thermodynamic and transport properties-REFPROP, Version 10.0, National Institute of Standards and Technology. *Stand. Ref. Data Program Gaithersburg* **2018**, 45–46. [CrossRef]
7. Qiu, G.; Zhu, S.; Wang, K.; Wang, W.; Hu, J.; Hu, Y.; Zhi, X.; Qiu, L. Numerical study on unsteady heat transfer and fluid flow in a closed cylinder of reciprocating liquid hydrogen pumps. *Int. J. Hydrogen Energy* **2023**, *48*, 30156–30169. [CrossRef]
8. Lai, T.; Yan, S.; Wang, Y.; Liu, X.; Qiang, M.; Ding, W.; Liu, Y.; Hou, Y. Numerical study on static performance of hydrodynamic bearing in high-speed liquid hydrogen centrifugal pump. *Int. J. Hydrogen Energy* **2023**, *48*, 1552–1567. [CrossRef]
9. Gao, H.; Gu, S.; Wang, C. Research status and key technical problems of high-pressure liquid hydrogen pump industry. *Nat. Gas. Ind.* **2024**, *44*, 166–177.
10. Wei, W.; He, Z.; Xing, Z. Overview of advances in the research of high-pressure liquid hydrogen pump. *Fluid Mach.* **2022**, *50*, 79–84.
11. Krishnadoss, R.; Dyrland, I.A.; Adams, T.A. Design and optimization of alcohol-ketone-hydrogen chemical heat pumps. *Comput. Chem. Eng.* **2025**, *199*, 109158. [CrossRef]
12. Xu, M.; Xin, F.; Li, X.; Huai, X.; Liu, H. Ultrasound promoted catalytic liquid-phase dehydrogenation of isopropanol for Isopropanol–Acetone–Hydrogen chemical heat pump. *Ultrason. Sonochem.* **2015**, *23*, 66–74. [CrossRef]
13. Ho, S.H.; Rahman, M.M. Three-dimensional analysis for liquid hydrogen in a cryogenic storage tank with heat pipe–pump system. *Cryogenics* **2008**, *48*, 31–41. [CrossRef]
14. Zhai, Q.; Lin, J.; Li, Y.; Han, D.; Wu, X. Analysis of new pump-thermal synergized liquid hydrogen refueling station system (exergy). *CIESC J.* **2025**, *76*, 5390–5401.
15. Li, Y.; Li, W.; Ji, L.; Huang, Y.; He, S.; Li, S.; Zhai, H.; He, J.; Li, X. Effect of suction temperature on the internal flow characteristics of hydrogen circulation pump. *Appl. Therm. Eng.* **2024**, *247*, 122949. [CrossRef]
16. Yim, W.; Yoon, J.; Cha, J.; Bong, U.; Hahn, S. A design study on 20 kW class axial flux motor with HTS field winding for 100 MPa liquid hydrogen pump. *Cryogenics* **2024**, *139*, 103829. [CrossRef]
17. Chen, Z.; Liu, H.; Wei, Z.; Lu, F.; Zhang, X. Research status and prospect of reciprocating liquid hydrogen pump. *Fluid Mach.* **2021**, *49*, 68–75.
18. Qiu, N.; Shang, X.; Liu, R.; Jin, P.; Gao, W. Analysis of the dynamic characteristics of the pump valve system of an ultra-high pressure liquid hydrogen reciprocating pump. *Energies* **2022**, *15*, 4255. [CrossRef]
19. Zhang, F.; Li, X.; Zhang, X.; Xiong, X.; Cui, X.; Cai, X.; He, G. Safety design of the piston rod seal structure for submerged high-pressure liquid hydrogen pump. *Clean. Energy* **2025**, *9*, 108–122. [CrossRef]
20. Ren, H.; Wu, W.; Yang, S.; Xie, X. Numerical investigation on leakage characteristics of labyrinth seal for cavitation flow in the liquid hydrogen piston pump. *Clean. Energy* **2025**, *9*, 147–157. [CrossRef]
21. Sandoval, R.; Karplus, V.J.; Paltsev, S.; Reilly, J.M. Modelling prospects for hydrogen-powered transportation until 2100. *J. Transp. Econ. Policy (JTEP)* **2009**, *43*, 291–316. [CrossRef]
22. Chen, Z.; Zhao, Y.; Jia, Y.; Zheng, X.; Shao, G.; Li, Y.; Liu, M.; Shi, J.; Gu, C. The impacts of the hydrogen economy on climate: Current research and future projections to 2050. *Int. J. Hydrogen Energy* **2025**, *119*, 204–217. [CrossRef]

23. Staffell, I.; Scamman, D.; Abad, A.V.; Balcombe, P.; Dodds, P.E.; Ekins, P.; Ward, K.R. The role of hydrogen and fuel cells in the global energy system. *Energy Environ. Sci.* **2019**, *12*, 463–491. [CrossRef]
24. Johnson, N.; Liebreich, M.; Kammen, D.M.; Ekins, P.; McKenna, R.; Staffell, I. Realistic roles for hydrogen in the future energy transition. *Nat. Rev. Clean. Technol.* **2025**, *1*, 351–371. [CrossRef]
25. Bockris, J.O.M. A hydrogen economy. *Science* **1972**, *176*, 1323. [CrossRef]
26. IEA. Global Hydrogen Review 2024. Available online: https://www.iea.org/reports/global-hydrogen-review-2024 (accessed on 10 May 2026).
27. Wei, X.; Shi, X.; Li, Y.; Ma, H.; Ban, S.; Liu, X.; Yang, C. Analysis of the European energy crisis and its implications for the development of strategic energy storage in China. *J. Energy Storage* **2024**, *82*, 110522. [CrossRef]
28. Terlouw, T.; Rosa, L.; Bauer, C.; McKenna, R. Future hydrogen economies imply environmental trade-offs and a supply-demand mismatch. *Nat. Commun.* **2024**, *15*, 7043. [CrossRef] [PubMed]
29. Zeng, J.; Bao, R.; McFarland, M. Clean energy substitution: The effect of transitioning from coal to gas on air pollution. *Energy Econ.* **2022**, *107*, 105816. [CrossRef]
30. Zhou, N.; Price, L.; Yande, D.; Creyts, J.; Khanna, N.; Fridley, D.; Franconi, E. A roadmap for China to peak carbon dioxide emissions and achieve a 20% share of non-fossil fuels in primary energy by 2030. *Appl. Energy* **2019**, *239*, 793–819. [CrossRef]
31. Tarhan, C.; Çil, M.A. A study on hydrogen, the clean energy of the future: Hydrogen storage methods. *J. Energy Storage* **2021**, *40*, 102676. [CrossRef]
32. Okonkwo, P.C.; Belgacem, I.B.; Zghaibeh, M.; Tlili, I. Optimal sizing of photovoltaic systems based green hydrogen refueling stations case study Oman. *Int. J. Hydrogen Energy* **2022**, *47*, 31964–31973. [CrossRef]
33. IEA. *Global Hydrogen Review 2025*; International Energy Agency: Paris, France, 2025.
34. Hydrogen Patents for a Clean Energy Future. Available online: http://iea.li/hydrogen-innovation (accessed on 10 May 2026).
35. Berrada, A.; Laasmi, M.A. Technical-economic and socio-political assessment of hydrogen production from solar energy. *J. Energy Storage* **2021**, *44*, 103448. [CrossRef]
36. Sherif, S.A.; Zeytinoglu, N. Liquid hydrogen: Potential, problems, and a proposed research program. *Int. J. Hydrogen Energy* **1997**, *22*, 683–688. [CrossRef]
37. Terlouw, T.; Moretti, C.; Harpprecht, C.; Sacchi, R.; McKenna, R.; Bauer, C. Global greenhouse gas emissions mitigation potential of existing and planned hydrogen projects. *Nat. Energy* **2025**, *10*, 1503–1515. [CrossRef]
38. Li, J.; Ramteke, A.; Youn, E.; Hansen, E.; Kratschmar, K.; Prakash, A.; Ku, A.Y. Liquid pump-enabled hydrogen refueling system for heavy duty fuel cell vehicles: Pump performance and J2601-compliant fills with precooling. *Int. J. Hydrogen Energy* **2021**, *46*, 22018–22029. [CrossRef]
39. Petitpas, G.; Aceves, S.M. Liquid hydrogen pump performance and durability testing through repeated cryogenic vessel filling to 700 bar. *Int. J. Hydrogen Energy* **2018**, *43*, 18403–18420. [CrossRef]
40. Xiang, L.; Tan, Y.H.; Chen, H.; Xu, K. Numerical simulation of cryogenic cavitating flow in LRE oxygen turbopump inducer. *Cryogenics* **2022**, *126*, 103540. [CrossRef]
41. IEA. Global Hydrogen Review 2022. Available online: www.iea.org (accessed on 10 May 2026).
42. Wang, X.; Li, K.; Liu, G.; Wang, H.; Sun, B.; Zhang, C. Collaborative optimization of hydrogen energy systems: A game-theoretic integration of production, usage and refueling in cross-sectoral scenarios. *Appl. Energy* **2025**, *398*, 126450. [CrossRef]
43. Al-Orabi, A.M.; Osman, M.G.; Sedhom, B.E. Analysis of the economic and technological viability of producing green hydrogen with renewable energy sources in a variety of climates to reduce CO_2 emissions: A case study in Egypt. *Appl. Energy* **2023**, *338*, 120958. [CrossRef]
44. Xiang, Z.; Li, R.; Zuo, Y. 2060 World Energy Development Trend and China's Energy Transition Path: Simulation Analysis Based on Benchmark, In-depth Game and Comprehensive Cooperation Scenario. *World Pet. Ind.* **2025**, *32*, 1–11. [CrossRef]
45. Global Hydrogen Review 2023. Available online: https://www.iea.org/reports/global-hydrogen-review-2023 (accessed on 10 May 2026).
46. Wang, Z. Assessing the economic feasibility of hydrogen generation from renewable energy sources. *Int. J. Hydrogen Energy* **2025**, *152*, 149940. [CrossRef]
47. Levikhin, A.A.; Boryaev, A.A. Physical properties and thermodynamic characteristics of hydrogen. *Heliyon* **2024**, *10*, e36414. [CrossRef]
48. Zhang, X.; Zhao, D.; Ma, S.; Zhang, X.; Yan, K. Thermal-mechanical coupled interaction of angular contact ball bearing considering combined deformation. *Tribol. Int.* **2025**, *212*, 110994. [CrossRef]
49. Yan, S.; Lai, T.; Qiang, M.; Zhao, Q.; Ding, W.; Liu, Y.; Hou, Y. Research on the cavitation characteristics and structural optimisation of spiral grooved thrust bearing lubricated by liquid hydrogen. *Lubr. Sci.* **2024**, *36*, 241–258.
50. Brennen, C.E. *Cavitation and Bubble Dynamics*; Cambridge University Press: Cambridge, UK, 2014.
51. Jacobsen, R.T.; Penoncello, S.G.; Lemmon, E.W. *Reference Data for the Thermophysical Properties of Cryogenic Fluids (NASA/CR—2007-215162; NIST IR 6643)*; National Institute of Standards and Technology: Gaithersburg, MD, USA, 2007.

52. Hammer, M.; Bauer, G.; Stierle, R.; Gross, J. Classical density functional theory for interfacial properties of hydrogen, helium, deuterium, neon, and their mixtures. *J. Chem. Phys.* **2023**, *158*, 104107. [CrossRef]
53. Debenedetti, P.G. *Metastable Liquids: Concepts and Principles*; Princeton University Press: Princeton, NJ, USA, 1997.
54. Batchelor, G.K. *An Introduction to Fluid Dynamics*; Cambridge University Press: Cambridge, UK, 2000.
55. Ma, C.; Zhang, J.; Wang, X.; Meng, H.; Guo, S. Thermal Insulation Optimization of Turbocharger Bearing Housing: A Comparative Study on Heat Shield Configurations and Ventilation Strategies. *Energy* **2025**, *332*, 137185. [CrossRef]
56. Xu, Z.; Tan, H.; Wu, H. Experimental and simulation study on transient heat transfer behaviour of multi-layer insulation for cryogenic vessels. *Cryogenics* **2025**, *150*, 104136. [CrossRef]
57. Shu, Q.S.; Demko, J.A.; Fesmire, J.E. Developments in advanced and energy saving thermal isolations for cryogenic applications. In *IOP Conference Series: Materials Science and Engineering*; IOP Publishing: Bristol, UK, 2015; Volume 101, p. 012014.
58. Barron, R.F.; Nellis, G.F. *Cryogenic Heat Transfer*; CRC Press: Boca Raton, FL, USA, 2017.
59. Ruutu, V.M.H.; Eltsov, V.B.; Gill, A.J.; Kibble, T.W.B.; Krusius, M.; Makhlin, Y.G.; Xu, W. Vortex formation in neutron-irradiated superfluid 3He as an analogue of cosmological defect formation. *Nature* **1996**, *382*, 334–336. [CrossRef]
60. Maris, H.J.; Xiong, Q. Nucleation of bubbles in liquid helium at negative pressure. *Phys. Rev. Lett.* **1989**, *63*, 1078. [CrossRef]
61. Cengel, Y.A.; Boles, M.A. *Thermodynamics An Engineering Approach*, 8th ed.; McGraw-Hill Education: New York, NY, USA, 2014.
62. Bergman, T.L. *Fundamentals of Heat and Mass Transfer*; John Wiley & Sons: Hoboken, NJ, USA, 2011.
63. Hord, J. *Cavitation in Liquid Cryogens. 2: Hydrofoil*; NASA: Washington, DC, USA, 1973.
64. Ezzatneshan, E.; Salehi, A.; Vaseghnia, H. Numerical study on collapsing cavitation bubble dynamics in cryogenic fluids. *Cryogenics* **2024**, *141*, 103879. [CrossRef]
65. Zhang, X.B.; Qiu, L.M.; Gao, Y.; Zhang, X.J. Computational fluid dynamic study on cavitation in liquid nitrogen. *Cryogenics* **2008**, *48*, 432–438. [CrossRef]
66. Chen, T.; Wang, G.; Huang, B.; Wang, K. Numerical study of thermodynamic effects on liquid nitrogen cavitating flows. *Cryogenics* **2015**, *70*, 21–27. [CrossRef]
67. Dular, M.; Petkovšek, M. Cavitation erosion in liquid nitrogen. *Wear* **2018**, *400*, 111–118. [CrossRef]
68. Wang, Z.; Cheng, H.; Luo, X.; Ji, B. Multiscale numerical investigation of bubble distribution characteristics and cavitation erosion risk evolution with special emphasis on the influence of cavitation number. *Ocean Eng.* **2025**, *321*, 120398. [CrossRef]
69. He, X.; Peng, H.; Zhang, J. A lattice Boltzmann investigation of liquid viscosity effects on the evolution of a cavitation bubble attached to chemically patterned walls. *Phys. Fluids* **2023**, *35*, 093303. [CrossRef]
70. Lin, X.; Wang, S.; Jiang, S.; Zhang, S. Dynamic characteristics of high-speed water-lubricated spiral groove thrust bearing based on turbulent cavitating flow lubrication model. *Chin. J. Mech. Eng.* **2022**, *35*, 13. [CrossRef]
71. Kleinstreuer, C. *Two-Phase Flow: Theory and Applications*; Routledge: London, UK, 2017.
72. Reynolds, O., IV. On the theory of lubrication and its application to Mr. Beauchamp tower's experiments, including an experimental determination of the viscosity of olive oil. *Philos. Trans. R. Soc. Lond.* **1886**, *177*, 157–234. [CrossRef]
73. Cameron, A.G.W. *The Principles of Lubrication*; John Wiley & Sons Inc.: Hoboken, NJ, USA, 1966.
74. Taylor, G.I. Cavitation of a viscous fluid in narrow passages. *J. Fluid Mech.* **1963**, *16*, 595–619. [CrossRef]
75. Gumerov, N.A. Dynamics of vapor bubbles with nonequilibrium phase transitions in isotropic acoustic fields. *Phys. Fluids* **2000**, *12*, 71–88. [CrossRef]
76. Murai, Y.; Oiwa, H. Increase of effective viscosity in bubbly liquids from transient bubble deformation. *Fluid Dyn. Res.* **2008**, *40*, 565. [CrossRef]
77. Sweeny, K.H.; Geckler, R.D. The rheology of suspensions. *J. Appl. Phys.* **1954**, *25*, 1135–1144. [CrossRef]
78. Schramm, L.L. *Emulsions, Foams, Suspensions, and Aerosols: Microscience and Applications*; John Wiley & Sons: Hoboken, NJ, USA, 2014.
79. Wei, C.; Wang, W.; Xu, J.; Liu, X.; Liu, K. Transient instability characteristics of fluid film bearings induced by bubble inclusion. *Phys. Fluids* **2024**, *36*, 063106. [CrossRef]
80. Yu, X.; Feng, Y.; Gao, W.; Shi, G.; Li, S.; Chen, M.; Jiang, H. Study on lubrication performance of hydrostatic clearance oil film considering multi-factor coupling. *Int. J. Hydrogen Energy* **2022**, *47*, 40083–40098. [CrossRef]
81. Xie, F.W.; Zheng, X.D.; Sheng, G.; Sun, Q.; Agarwal, R.K. Numerical investigation of cavitation effect on two-phase oil film flow between a friction pair in hydro-viscous drive. *Proc. Inst. Mech. Eng. Part C J. Mech. Eng. Sci.* **2018**, *232*, 4626. [CrossRef]
82. Cui, G.; Shang, X.; Li, S.; Cui, K.; Xu, Q.; Chen, Y.; Shi, H. Coupled effects of viscosity-temperature characteristics and cavitation on oil film torque transmission in silicone oil fan clutches. *Int. J. Therm. Sci.* **2026**, *220*, 110431. [CrossRef]
83. Xie, F.W.; Zhu, J.; Tong, Y.W.; Zhang, B.; Agarwal, R.K. Numerical study on cavitation in oil film and its impact on transferred torque. *Recent Pat. Mech. Eng.* **2017**, *10*, 153. [CrossRef]
84. Li, Z.H.; Zuo, Z.G.; Qian, Z.D. Diffusion-driven periodic cavitation bubbling from a Harvey-type crevice in shear flows. *Phys. Fluids* **2023**, *35*, 2112. [CrossRef]

85. Wang, Q.L.; Zhang, X.B.; Wang, D.G.; Cui, H.; Zhang, S.; Wang, J. Numerical simulation and experimental investigation on the thermal-fluid-solid multiphysical field coupling characteristics of wet friction pairs considering cavitation effect. *Appl. Therm. Eng.* **2025**, *260*, 124955. [CrossRef]
86. Yan, S.; Zhao, Q.; Lai, T.; Hou, Y. Effect of micro-clearance structure on the collapse of individual liquid hydrogen bubbles. *Energy Storage Sav.* **2024**, *3*, 231–241. [CrossRef]
87. Mayer, E. *Mechanical Seals*; Butterworth-Heinemann: Oxford, UK, 2013.
88. Gupta, R.; Prakash, J.; Miglani, A.; Kankar, P.K. On the Validity of Parallel Plate Assumption for Modelling Leakage Flow Past Hydraulic Piston-Cylinder Configurations. In *Intelligent Prognostics for Engineering Systems with Machine Learning Techniques*; CRC Press: Boca Raton, FL, USA, 2023; pp. 73–90.
89. Yamane, K.; Nakamura, S.; Nosset, T.; Furuhama, S. A study on a liquid hydrogen pump with a self-clearance-adjustment structure. *Int. J. Hydrogen Energy* **1996**, *21*, 717–723. [CrossRef]
90. Balachandran, G.; Balasubramanian, V. Stainless steel processing to meet advanced applications. *Adv. Mater. Res.* **2013**, *794*, 135–158. [CrossRef]
91. Liao, Z.Y.; Zhang, J.S.; Zhao, J.Q.; Yang, G.; Kong, R.Z. Research progress of hydrogen-resistant steels used in ultra-high pressure hydrogen environment. *J. Iron Steel Res.* **2023**, *35*, 1053–1064.
92. Michler, T.; San Marchi, C.; Naumann, J.; Weber, S.; Martin, M. Hydrogen environment embrittlement of stable austenitic steels. *Int. J. Hydrogen Energy* **2012**, *37*, 16231–16246. [CrossRef]
93. Ren, H.Y.; Yang, S.Q.; Wu, W.; Xie, X.J. Numerical investigation on transient sealing performance of square labyrinth seal in a liquid hydrogen piston pump. In *IOP Conference Series: Materials Science and Engineering*; IOP Publishing: Bristol, UK, 2025; Volume 1327, p. 012065.
94. Coleman, T.S.; Aghdam, K.H. Piston Seal Assembly with Controlled Leakage. U.S. Patent 10,316,837 B2, 11 June 2019.
95. Qiu, N. Structural Design and Heat Transfer Research of the Hydraulic End of a High-Pressure Liquid Hydrogen Pump. Master's Thesis, China Academy of Launch Vehicle Technology, Beijing, China, 2022.
96. Huang, C.; Li, L.; Yan, J.; Wu, J.; Dou, J.; Shi, Y.; Wang, J. Enhancing stress corrosion resistance in austenitic stainless steel through low-temperature oxy-nitriding surface modification: Investigation on H2S-induced phenomenon. *Surf. Coat. Technol.* **2024**, *478*, 130429. [CrossRef]
97. Michler, T.; Naumann, J. Coatings to reduce hydrogen environment embrittlement of 304 austenitic stainless steel. *Surf. Coat. Technol.* **2009**, *203*, 1819–1828. [CrossRef]
98. Wang, Y.; Xiong, L.; Feng, D.; Zhang, H.; Zhao, S.; Guo, Y. Research on the process performance of scroll forming by semi-solid forging procedure for scroll hydrogen recirculating pump. *Int. J. Hydrogen Energy* **2024**, *66*, 445–457. [CrossRef]
99. Li, D.; Ren, Z.; Li, Y.; Gong, R.; Wang, H. Thermodynamic effects on the cavitation flow of a liquid oxygen turbopump. *Cryogenics* **2021**, *116*, 103302.
100. Yu, A.; Wang, Y.; Song, F.; Li, Z.; Tang, Q. Numerical study of the entropy production characteristics in cryogenic liquid nitrogen cavitating flow. *Int. Commun. Heat. Mass. Transf.* **2022**, *133*, 105963. [CrossRef]
101. Xu, S.; Zhu, D.; Wang, C. Study on static heat leakage of liquid hydrogen pump for liquid hydrogen refueling station. *Vac. Low Temp.* **2024**, *30*, 424–428.

Disclaimer/Publisher's Note: The statements, opinions and data contained in all publications are solely those of the individual author(s) and contributor(s) and not of MDPI and/or the editor(s). MDPI and/or the editor(s) disclaim responsibility for any injury to people or property resulting from any ideas, methods, instructions or products referred to in the content.